Development and application of a compact and simple wind tunnel for blown sand experiment

（飛砂実験のための小型簡易風洞の開発とその応用）

Liu Jiaqi

United Graduate School of Agricultural Sciences,

Tottori University, Japan

2018

A thesis submitted in partial fulfillment of

the requirements for the degree of

Doctor of Philosophy

(Global Arid Land Science)

Acknowledgements

I would like to take this opportunity to express my gratitude to the following people for their extensive and invaluable help and support during my thesis writing. First and foremost, my sincerest thanks go to my supervisor, Professor Reiji Kimura, for his devoted support, constructive suggestions and endless patience with my writing. Without his guidance and encouragement, I would have never been able to complete my thesis. His academic enthusiasm and charming personality have enlightened me not only in this thesis but also in my future study and life.

I warmly thank my all colleagues at the Division of Climatology and water Resources, ALRC, for their kind cooperation, support, comments and help.

I am also very grateful to all those at the ALRC office, especially Mrs. Yonehara and others who were always so helpful and provided me with their assistance throughout my dissertation.

I would like to express my appreciation to my friends (too many to list here but you know who you are!) for providing support and friendship that I needed.

Finally, none of this would have been at all possible without the love and support that my family has given me. I am very grateful for my parents, Liu Jianguo and Wang Dongguo. Their understanding and their love encouraged me to work hard and to continue pursuing a Ph.D. project abroad. Their firm and kind-hearted personality has affected me to be steadfast and never bend to difficulty. They always lets me know that they are proud of me, which motivates me to work harder and do my best. Finally, special thanks to my wife, Zhang Yuwei, her understanding, and support throughout this process has been nothing short of incredible. Thank you for always believing in me and for never failing to bring a smile to my face when I needed it most. Thank you.

Liu Jiaqi

March 2018

I dedicate this thesis to

my family, my wife, and all of my friends

for their constant support and unconditional love.

With all my love

CONTENTS

List of symbols

Symbol	Explanation	SI Unit
ρ	air density	kg m^{-3}
δ	represents the thickness of the boundary layer	m
b	represents the width of the spires	m
u	wind speed	m s^{-1}
u_z	threshold wind speed	m s^{-1}
u_*	friction velocity	m s^{-1}
a	represents the exponent (=0.1)	-
H	represents the height of the wind tunnel (=0.5 m)	-
D	represents the spacing between the blocks(=0.05m)	-
d	the median particle size of sand	m
ρ_s	the density of sand (=2.65 x $10^3 kg/m^3$)	-
z_0	roughness length	m
k	von Karman's constant (= 0.4)	-
z	measurement height	m
d	zero plane displacement	m
t_0	the measurement time (=1s)	-

List of Figures

List of Tables

1. Introduction

1.1 General background

Currently, deserts cover 31,400,000 square kilometers of the earth's surface. In the past 20 years, desert regions have been expanding by an area of approximately 50,000 to 70,000 square kilometers per year due to the global warming. The expansion of desert areas causes frequent occurrences of sandstorms. Sandstorms affect an increasingly wide area every year, affecting several billion people and causing up to 42 billion dollars of economic damage. In recent years, sand drift is occurring more and more often in China(Kara Jean Hill, 2011). Afflicted regions are distributed over a wide area, and the extent of damage has been increasing as well. According to statistics, the frequency of occurrence of strong sand drifts was 5 times in the 1950s, 8 times in the 1960s, 13 times in the 1970s, 14 times in the 1980s, and 23 times in the 1990s. These statistics clearly demonstrate that the frequency has been increasing(Kara Jean Hill, 2011).

In order to mitigate damage caused by sand drift, it is first necessary to identify the factors that cause this phenomenon. Scientists are hopeful that it will be possible to apply the results of this research and develop technologies for suppressing sand drifts. However, since experiments conducted outdoors are hampered by adverse measurement conditions due to irregular changes in the wind direction, it is difficult for researchers to analyze how sand drift occurs. On the other hand, conducting experiments in wind tunnels allows researchers to analyze the sand drift phenomenon more easily. However, it is difficult to recreate conditions similar to natural environments using wind tunnels. Generation of boundary layers is one example.

In order to obtain a thick boundary layer in a wind tunnel environment, a long settling chamber in the direction of the flow is needed, which makes it necessary to have large scale facilities as well. Therefore, researchers have investigated various methods for achieving flows with properties that approximate those of atmospheric turbulent boundary layers within relatively short distances (Erie, 1978). In general, in order to form boundary layers in short settling chambers, boundary layers are formed by using

screens that are made of horizontal rods with spacings that are varied in the height direction (Kajiyama, 1993). Since this method requires large cross-sectional areas (horizontal width × vertical width), this method is not suitable for small-scale wind tunnels. In other methods, the boundary layer is considered as a shear field that is flowing along the wall surface. In these methods, methods for generation of a boundary layer are treated as methods for generating shear flows. Shear flows are generally formed by using meshes with apertures that are varied in the mainstream direction and direction perpendicular to the flow, wire nets that are bent into appropriate shapes, and honeycomb meshes of different lengths. However, it is difficult to create strong turbulent components such as those found in turbulent boundary layers at the same time (Erie, 1978).

1.2 Objective

The goal of this research is to create thick turbulent boundary layers in settling chambers that are as short as possible using simple small-scale wind tunnels. We attempted to design and develop a low-cost small-scale simple wind tunnel in which the stability of the horizontal profile of the wind velocity is maintained while forming a boundary layer that is relatively thick by using the two types of turbulence generators discussed by Counihan (1969) and Standen (1972) and the empirical formulas published by Irwin (1981).

2. Effect of blown sand mechanism on wind tunnel design

2.1 Effect of blown sand on wind tunnel design

When the soil-corrosive particles are removed from the ground under the action of wind, the transport will be carried out through three kinds of movement forms, such as, which mainly depend on the size of the particles, as shown in Fig. 2.1. "Saltation" means a continuous jump on the ground by a medium sized particle (particle size range 0.05~0.5 mm). They are very easy to ascend from the ground, but cannot be suspended; the jump height is generally less than lm（Qi and Wang, 1996）. "Surface creep" refers to the large particles (particle size generally under the l~2mm) in the air or other particles driven, along the surface of the rolling or sliding. "Suspension" refers to the very fine particles (diameter less than 0.1 mm) in a suspended state and with the airflow movement. A sandstorm is a long-range movement of a large number of suspended particles. In general, each of these three forms of motion occurs at the same time in each wind erosion phenomenon, and the transition is the most important form of movement of particles. This is because: (1) most of the soil particles move in the saltation mode. Studies have shown that 55~70 % soil particles move in saltation, 3~38% moves in suspension, and only 7~25% move in surface creep (Qi and Wang, 1996). The field observation of Wu Zheng and Ling (1965) also shows that, with the increase of wind speed, the proportion of the saltation in the pneumatic conveying sand increases slightly, but the change is not big, and the average accounts for about 3/4 (Wu and Ling, 1965). (2) A large number of surface creep and suspension cannot occur without the saltation. As for the suspended transport of sand grains, according to the study of Bagnold, the amount of sediment transported in suspended state is less than 5% of the total sediment transport (Qi and Wang, 1996). The transport form of the sand grains determines the structure of the wind-blown sand flow, which is the vertical distribution of the sand particle in the sand layer. Wang (1994) and Dong (1995) have summed up many studies, the results show that 90% of the sand grains on the surface of the soil are transported in

the height range from the ground to the CM, while the flow rate within the 0-5cm height is 60-80% (Qi and Wang, 1996). Butterfield (1999) used the High Resolution Optical Sensor and found that the sediment transport in the height range of the near surface 19mm accounted for about 80% of the total sediment load (Butterfield, 1999). Thus, the sand movement is a kind of sand transport phenomenon which is close to the ground 30 cm height range. The sand movement within 30 cm near the surface ground is important during the sand transport phenomenon. This altitude range provides an important reference for the altitude design of the experimental section of the blown sand wind tunnel.

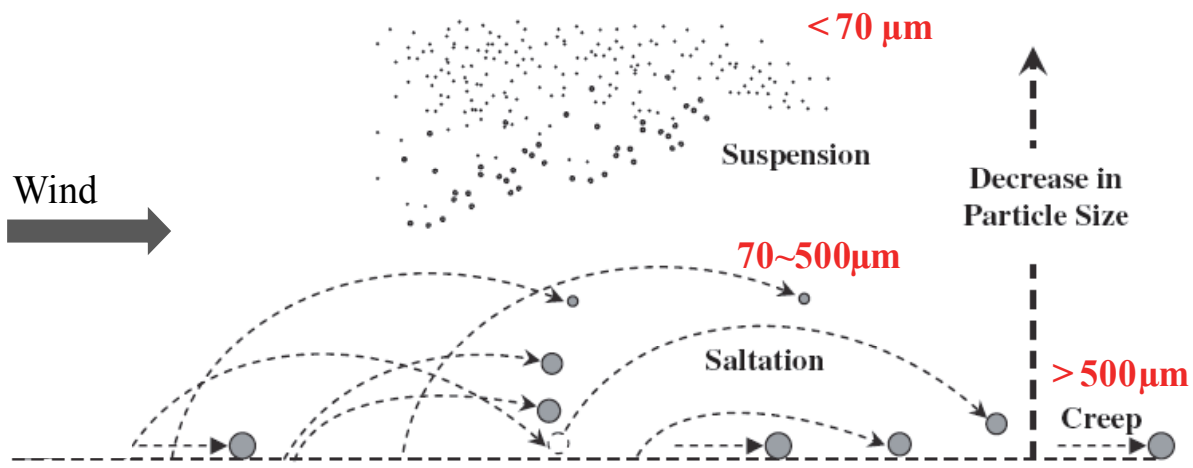

Fig. 2.1. An illustration of creep, saltation and suspension of soil particles (cited from Shao, 2008).

2.2 Starting process of soil particles and determination of wind speed threshold parameters

The starting process of soil-corrosive particles is the first step in the process of wind erosion, and the determination of wind speed parameters is one of the important contents of wind erosion research. Experimental observation shows that only when the wind speed exceeds a certain critical value, soil particles can be induced to rise from the surface and form wind erosion. The observation also shows that there are two different threshold wind speed (Foucaut and Stanislas, 1996): (1) The starting wind speed of the fluid, which is the minimum wind speed that the soil particles start to move with the direct action of the grainy wind; (2) The impact of the starting wind speed, also known as dynamic valve value. It is the minimum wind speed at which the soil particles start to move when there is an auxiliary effect from the upper direction to jump particle impact. The physical meaning of the critical value of the fluid starting wind speed and the impact starting velocity is explained in the view of the wind tunnel experiment as follows (Dong and Li, 1995). When the sand in the wind tunnel to start the experiment, always first with a basically sand-free air blowing through the sand, when the air velocity gradually increased to a certain value, the bed of sand on the surface began to move and produce sand flow, the wind speed is the sand of the fluid starting wind speed. Once the sand flows is formed, and then gradually reduce the wind speed to the starting velocity of the fluid, the sand flow does not stop until the wind speed drops to a certain value below the starting speed of the fluid, the sand flow is completely suspended, the wind speed is the impact of the sand. The threshold of the soil erosive particles is a characterization of soil wind erosion resistance, which is related to grain size, surface properties and water content. It can be seen that wind speed is an important parameter in wind tunnel experiment, the design of wind tunnel should be able to measure the wind speed of the experimental section, and the speed of air can be controlled and adjustable.

2.3 Design requirements of wind erosion wind tunnel by simulating atmospheric boundary layer

The wind velocity profile is an extremely important boundary condition to be satisfied in the simulation of atmospheric boundary layer, because the shape of wind velocity profile determines the interaction between wind and surface interface. Observation of the near-earth surface air velocity profile is necessary for wind tunnel experiment to simulate wind-blown wind tunnel. Wind tunnel simulation of wind-erosion problem is the most critical of wind speed profile simulation. A large number of studies have been reported (Gillette, 1978) for the study of wind velocity profiles in the near-surface atmospheric boundary layer. It is generally believed that the average wind velocity profile of the atmospheric boundary layer can be expressed either by a power-finger law or by logarithmic law.

The expression of a power-finger law is (Tan et al., 2013):

$$\frac{u}{u_r} = \left(\frac{z}{z_r}\right)^a \tag{1}$$

The expression of the logarithm law is White (1996). In neutral stratified atmosphere, the wind profile above uniform surface obeys the law of wall represented by the equation (Tan et al., 2013):

$$u_z = \left(\frac{u_*}{k}\right) ln\left(\frac{z}{z_0}\right) \tag{2}$$

where u_z is the wind velocity at height z, u_* is the friction velocity, k is von Karman constant (0.4) and z_0 is aerodynamic roughness length. When wind encounters and flows over a roughness length. When wind encounters and flows over a rough surface, the wind profile may be displaced upward by an addition of a displacement height term (d) in the Eq.(1) ,and thus the wind profile equation changes into:

$$u_z = \left(\frac{u_*}{k}\right) ln\left(\frac{z-d}{z_0}\right) \quad (3)$$

Gillies et al. (2007) showed that for surfaces with small roughness elements, d=0 when d « 2 m. Therefore, in this study, a value for d was not used in the calculation of u_*.The expression of the logarithm law is White (1996).

The power-exponent law is often used to express the wind velocity distribution of the large-scale atmospheric boundary layer, while the logarithm law is often used to express the wind velocity distribution of the atmospheric boundary layer in the near-surface layer (White, 1996). Theoretically, the wind tunnel simulation of the near-earth surface atmospheric boundary layer, as long as wind tunnel wind speed and surface roughness condition of wind tunnel are identical with the field wind speed and surface condition to be simulated. The development of logarithmic wind velocity profile through certain wind distance will be formed naturally. However, in practice, the wind distance required to obtain a well-developed wind speed profile in a wind tunnel is quite long. It means that the length of the inlet sampling area in the wind tunnel experimental section is quite long, which is not feasible in most practical situations. Cermak(1981) shows that the natural development thickness of the 0.5m boundary layer requires at least the development length of the 15m (Cermak, 1981). The movable wind-erosion wind tunnel with such a long experimental section is not acceptable in terms of cost, use and convenience of operation. Therefore, the design of movable wind-erosion wind tunnel must consider the method of artificially thickened boundary layer, so that it can correctly simulate the wind velocity profile of the atmospheric boundary layer near the surface of the bottom surface in the wind tunnel of the short experimental section. This is a key technical problem to be solved in the design of blown sand wind tunnel.

2.4 Technical development of wind field simulation of atmospheric boundary layer in wind tunnel

Wind erosion occurs only when a threshold value of the wind velocity is reached and this threshold depends on the soil surface features. The numerous studies have been done to examine the soil moisture effect on wind erosion since Chepil (1956), and it is a well-known fact that the threshold wind speed increases with soil moisture (Belly, 1964, Bisal and Hsieh. 1966, McKenna-Neuman and Nickling, 1989, Selah and Fryrear, 1995, Fe´can et al., 1999).

The method, passive simulation of wind tunnel flow field, was proposed in 1960. The most proposed method that using the interaction of rough plate, roughness element and baffler is the passive simulation of wind tunnel flow field. Cook found that the formation of turbulent boundary layer depends on the size, shape and spacing of roughness elements, when he used a grid and surface roughness elements to simulate the wind field. Counihan et al. firstly used wide in lower but narrow in upper wedge and rough hexahedral roughness elements to simulate neutral atmospheric boundary layer in wind tunnel systematically (Counihan, 1972). Irwin changed the wedge to a triangular shape, and suggested that non-triangular wedge has no apparent advantage compared with the triangular wedge (Irwin, 1981). Sill studied the relationship between the roughness elements size and arrangement pattern of cube and the roughness (Sill, 1988).

2.5 Introduction to wind field simulation of atmospheric boundary layer in wind tunnel

Wind field simulation of atmospheric boundary layer can be performed by two ways: one is natural simulation method, the other is artificial simulation method. In the natural simulation, simulated atmospheric boundary layer is uniformly and naturally formed on rough walls and it required a long test section, what's more, it usually takes more than 20 m. In addition, it also needs some artificial turbulence devices. Therefore, it is rarely used currently.

This paper mainly introduces the artificial simulation method. It is a kind of mainstream atmospheric boundary layer simulation method, which is popular all the world. So far, there are majority ways, such as curved networks, stick fence, curve section honeycomb and wedge roughness elements. There are two methods of artificial simulation according to the absence or presence of energy injection into wind tunnel test section: passive and active simulation.

(1) Passive simulation method

For passive simulation, grid, wedge, roughness elements, baffler and other devices are used for blocking the movement of the flow field in the wind tunnel, generating a gradient flow field in the height direction and forming a shear layer, finally, it forms turbulent swirl and a shear boundary layer. Besides, passive simulation apparatus does not require energy input. Because it can get energy from obstructing and interfering wind tunnel flow field that a portion of the kinetic energy of liquid in the wind tunnel was converted into the turbulent energy and achieving the simulation of atmospheric boundary layer.

The earliest passive simulation method is to use grid plate device system. It generates vortex from combination of some plates with different widths and space, which will be put on the wind field upstream to disturb magnetic wind. By adjusting the widths and space of the plates, it will form some turbulence with different intensities and integral scales. Besides, there is also a similar method, rod grid method, in which plates are replaced by round sticks. Oven and Cockrell formed linear distribution wind speed section and exponential distribution wind speed section, respectively, by rod grid

method. However, this method currently is rarely used.

So far, the most common method is wedge roughness elements passive simulation system. In this system, wedge and roughness elements are used to block the air movement in the flow field, but wedge has a greater impact. Wedge determines the general cross-sectional shape of the wind, especially for upper wind field, whereas it is difficult for roughness element, because it is limited by its height, its influence range is focused to a certain height. But, because the wind speed at the bottom of the atmospheric boundary layer is much bigger, thus, the bottom turbulence intensity is also considerable. Besides, most buildings located in the lower height part of the atmospheric boundary layer. Therefore, it is also important to use roughness elements rationally.

It is difficult to form a thick boundary layer for only roughness elements, so the effect of wedge on controlling the wind profile is very important. Further, the variation pattern of wedge along the height direction determines the characteristic scale of separation on the wedge surface, which control the upper turbulivity and turbulent integration scale. In comparison, the area of wedge windward plate determines the cross-section blocking rate of wind field, and then it directly determines the cross-sectional shape of the wind speed.

(2) Active simulation method

In active simulation method, appropriate frequency of mechanical energy is injected a flow field, to enhance the turbulent kinetic energy with low-frequency component, thereby improving the simulation of the power spectrum and the integration length and independently changing the average wind profile and turbulivity within a certain range. The turbulence boundary layer simulated in wind tunnel is mainly generated by the vortex generator. By comparing the wind speed spectrum and the target spectrum, the random signal of vortex generator can be reversely adjusted, so as to gradually approach to get the wind characteristic of the target atmospheric boundary layer. In a simple active simulation, a stationary vortex generator will undergo random vibration, then the mechanical energy is injected into the flow field to increase the turbulent energy, different turbulence integration scales can be obtained by controlling the waveform of vibration. State University used vibrating wing-grid for active

simulation, that is, by setting two rows of controllable vibrating wing-grids to randomly vibrate in a cycle, the cross-sections and dimensions of the turbulent boundary layer downstream can satisfy the contracting ratio wind tunnel experiment. The active control of the wind tunnel, multi-fan tunnel, is equipped with a fan array of frequency control technique, this method is the best wind tunnel solution to simulate the characteristic of atmospheric boundary layer wind field. This technique was developed in Japan as a better dynamic simulation technology based on the prototype of Teunissen's multi-jet wind tunnel (Cermak and Cochran, 1992), in the prototype, it consists of a 8*8 array of jet tubes, and each tube's inner diameter is about 6.2 mm and the jet velocity is controlled by a valve, the experimental section is only about 0.2 m * 0.2 m * 2.86 m. Figure 2.2 shows a multi-fan wind tunnel designed by, Japan, the jet device is composed of 9-row and 11-column array, i.e. a total of 99 fans, the test section size reaches 2.6 m * 1.8 m * 15.5 m. The rotational speed of each fan can be controlled independently by a computer for random fluctuation, a hot-wire anemometer can be used to measure the fluctuation velocity and its power spectrum downstream. After feedback and repeatedly and reversely adjusting for approximation, finally it can obtain a atmospheric boundary layer flow field that coincides with the characteristics of the target. This technology can simulate almost a wind velocity time series that is entirely consistent with the target wind field.

Fig 2.2 Multi-fan device in Miyazaki University

3. On the boundary layer formation of a small simple type wind tunnel

3.1 Wind tunnel structure

Figure 3.1 shows a diagram and a photograph of the wind tunnel used in this research. The wind tunnel that was used is a single-circuit open-return wind tunnel and is composed of a fan, settling chamber, and test section. The length of the wind tunnel is 8.25 m, and its cross section is 0.8 m × 0.5 m. The length of the settling chamber is 3.6 m, and the length of the test section is 1.8 m.

Considering the fact that sand drift in the natural environment is most vigorous at heights below 0.3 m (Abulaiti and Kimura, 2011), the height of the wind tunnel was chosen to be 0.5 m in order to keep the wind tunnel small. The width of the wind tunnel was set to be less than 1 m in order to keep the wind tunnel small, assuming that a wind layer that is affected by friction is formed in an area 0.2 m from the inner side of both walls（Yoshino et al., 1985）. The overall length of the wind tunnel and the lengths of the settling chamber and test section were chosen based on the outdoor wind tunnel of Tan and Zhang (2013) as a reference.

The exterior wall has a thickness of 0.8 cm and is made of acrylic. Acrylic was selected because it improves visibility of the condition of the sand drift as well as the process of the experiment. The thickness was chosen to be 0.8 cm because this thickness mitigates the degradation of the acrylic in our experience. The ceiling was designed to be removable so that it would be easy to set up the experiment.

The maximum output of the fan that was used in this experiment was 1.5 kW (Figure 3.2). The fan is equipped with an inverter (Figure 3.3), making it possible to change the wind velocity to according to the required wind velocity in the test section. The frequency can be adjusted from 0 Hz to 60 Hz, and the wind velocity of the wind created by the fan can be adjusted from 0 m/s to 12 m/s.

A hexagonal-type honeycomb (Figure 3.4) was placed at the exit of the fan. The purpose of the honeycomb is to straighten the flow of the turbulent air that is sent from

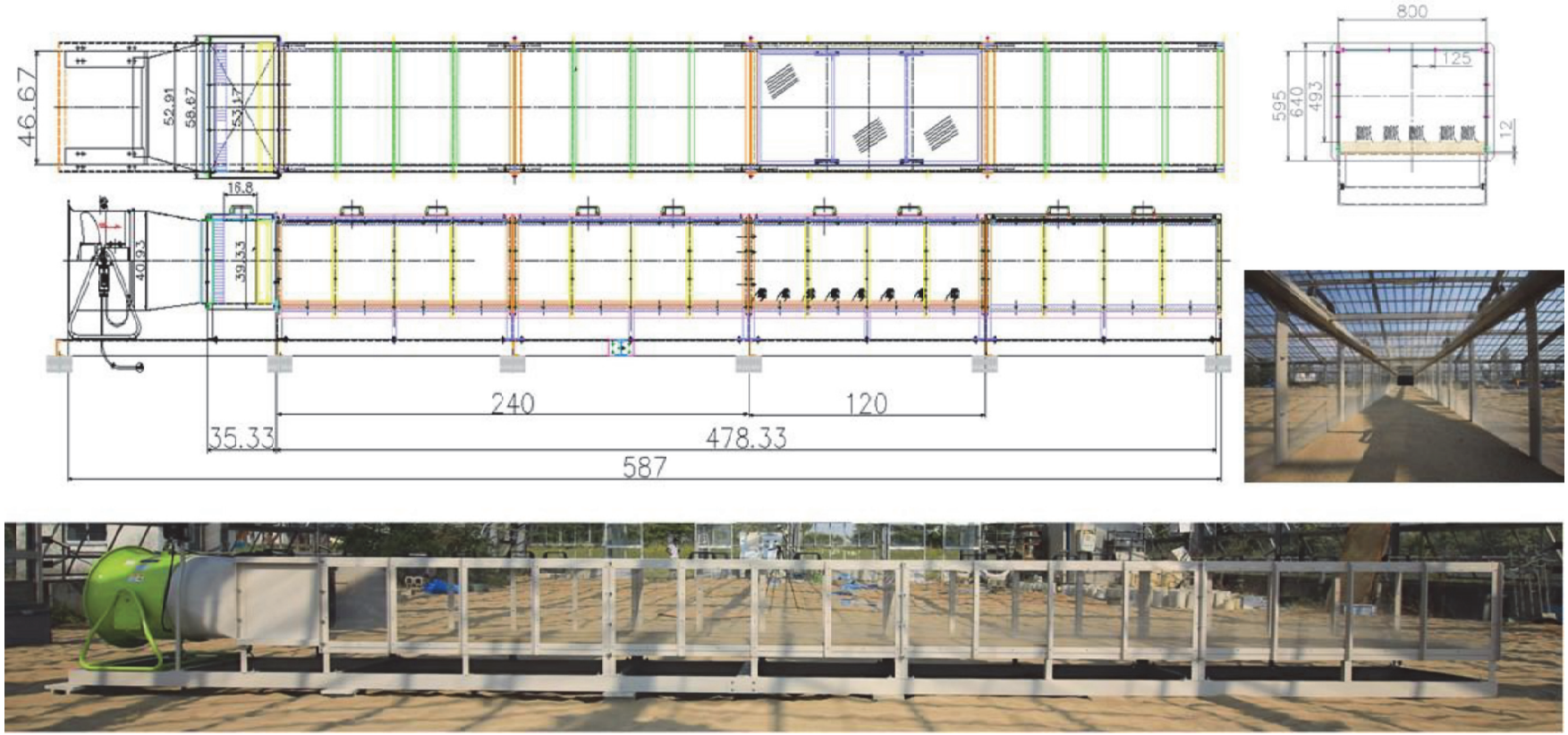

Fig 3.1 Schematic and actual photo of wind tunnel

Fig 3.2 Pictures of fan

Fig 3.3 Pictures of inverter

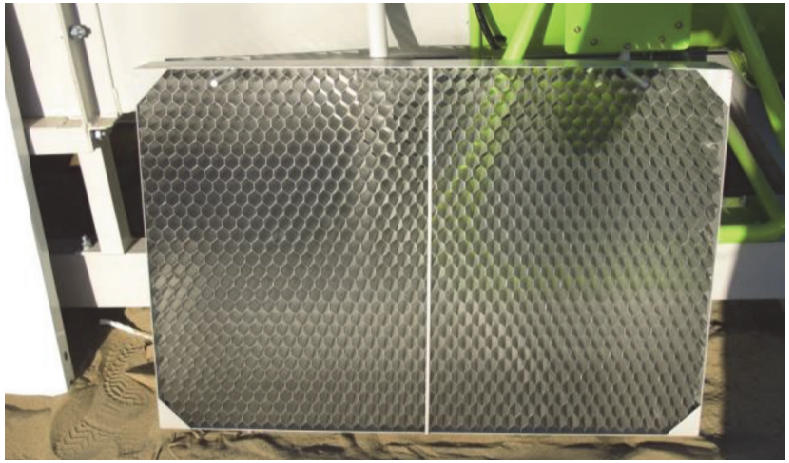

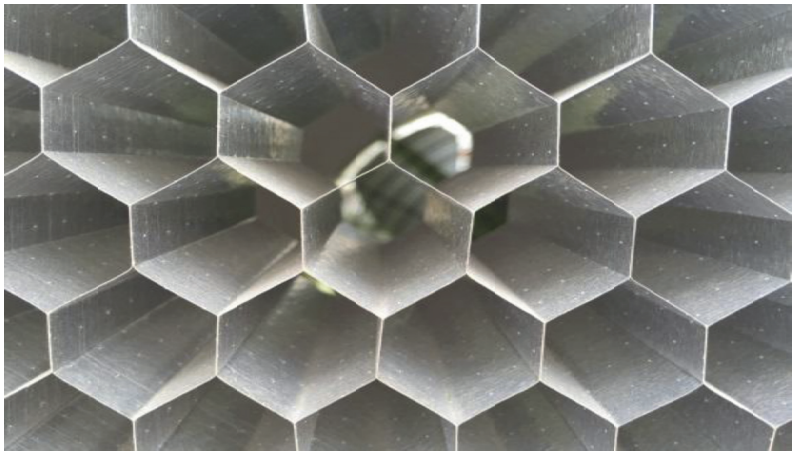

Fig 3.4 Pictures of honeycomb

the fan to flow in a constant direction. Increasing the length of the honeycomb results in more straightening of the air flow, but this also causes larger losses in the wind velocity. Decreasing the diameter of the honeycomb cells also results in deceased turbulence intensity. The honeycomb that was used in this research was made of aluminum and had a thickness of 0.2 cm, length of 8 cm, and diameter of 2 cm, which were chosen based on the results in Mehta (1977).

3.2 Wind velocity measurement method

In this research, experiments were performed with the mainstream wind velocity maintained at a constant value of 8 m/s. The wind velocity was measured using a pitot tube (Figure 3.5) anemometer that was fixed to a stand. Moving observations of the wind velocity in the vertical direction and horizontal direction were taken on the upwind side of test section. The measurement axis for the vertical direction was chosen to be at the center of the upwind side of the test section. The measurement was performed in the height range of 0.4 cm - 50 cm (2 cm measurement interval). The measurement axis for the horizontal direction was chosen to be at the upwind side of the test section as well. The measurement was performed at a height of 4 cm and in the range of 0.4 cm - 78 cm from the wall (2 cm measurement interval). The measurement interval was chosen to be 2 cm based on the sensor specifications. The data was recorded at an interval of 1 second. 30 seconds of data were averaged and used for the analysis (Figure 3.6).

In order to measure the wind velocity profile in the vertical and horizontal directions for the case in which the ground is covered in sand, the measurement was taken with a wooden board with sand stuck onto it placed on the floor.

Fig 3.5 Picture of pitot tube

Fig 3.6 Picture taken from wind tunnel observation site

3.3 Boundary layer formation method and design of turbulence generator

3.3.1 Boundary layer formation method

Methods for reproducing boundary layers in wind tunnels can be categorized into two types: ① Methods in which the boundary layer is formed naturally, and ② methods in which the boundary layer is formed artificially. In methods in which the boundary layer is formed naturally, the boundary layer is formed naturally by walls of the same roughness. In order to form a boundary layer of thickness 0.5 - 1.0 m, a settling chamber of length 20 - 30 m is required. Considering the installation costs, such a settling chamber would be too long, making this method unrealistic.

In methods in which the boundary layer is formed artificially, the boundary layer is formed by placing turbulence generators in the settling chamber. In this experiment, we chose to design and deploy turbulence generators in order to adjust the boundary layer. In this method, the turbulence generators receive the wind that is sent from the fan and artificially generate an exponential wind velocity profile along the height profile of the turbulence generators (Figure 3.7). In this case, a logarithmic distribution of the wind velocity is generated in the vertical direction, even when the settling chamber is short.

The turbulence generators that were used in this experiment include both spires, which are pyramid-shaped columns, and roughness blocks arranged along the floor.

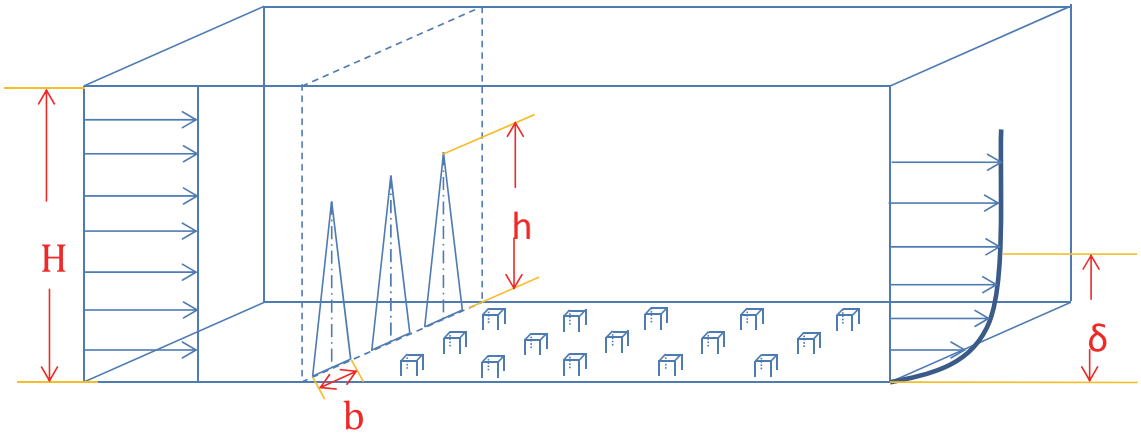

Fig 3.7 Schematic diagram of the turbulence generator installation method

3.3.2 Design of spires and roughness blocks

The sizes of the spires and the roughness blocks must be determined based on the size of the wind tunnel. According to the research results presented in Irwin (1981), the height and width of the spires can be calculated using the following equations.

$$h = 1.39\delta/(1+a/2) \tag{4}$$

$$\frac{b}{h} = 0.5(1+\frac{a}{2})\frac{H}{\delta}\times\frac{\varphi}{1+\varphi} \tag{5}$$

$$\varphi = \frac{\beta}{(1-\beta)^2}(\frac{2}{(1+2a)}+\beta-\frac{1.13a}{(1+a)(1+a/2)}) \tag{6}$$

$$\beta = \frac{\delta}{H}\times\frac{a}{1+a} \tag{7}$$

Here, h represents the height of the spires (m), δ represents the thickness of the boundary layer (set to be 0.3 m in this research), b represents the width of the spires (m), a represents the exponent (set to the value for a sandy surface, or 0.1, in this research), and H represents the height of the wind tunnel (0.5 m). Based on the calculation results, the value of h is 0.23 m, and the value of b is 0.024 m (Figure 3.8a). In the research results presented in Irwin (1981), the spacing of the spires was set to be half of their height. However, in this research, the spacing of the spires was set to be 0.125 m, and 6 spires were installed (Figure 3.8b).

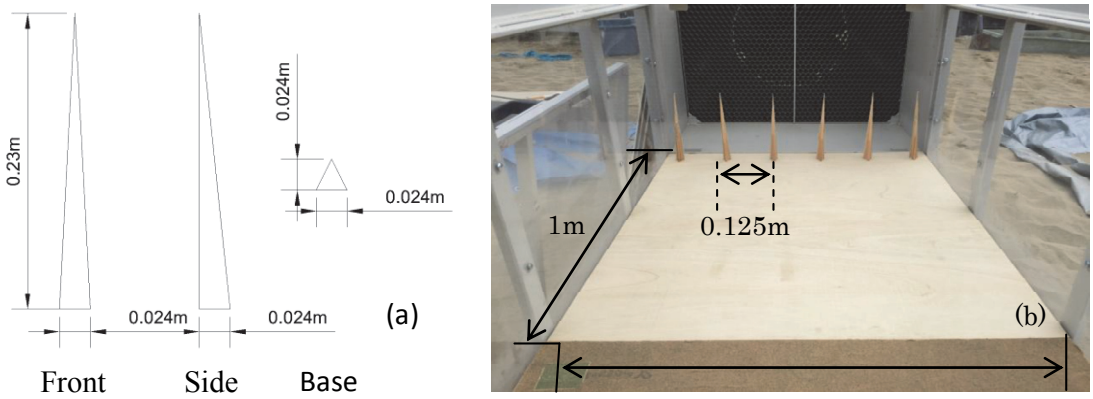

Figure 3.8 Schematic of spire (a) and pictures of installation (b)

In this experiment, the boundary layer was generated artificially in order to avoid using a long settling chamber that would have been required in order to form the

boundary layer naturally. However, if the length of the settling chamber is made short, it is difficult to make the profile of the wind velocity constant in the horizontal direction. Therefore, in this research, cubic roughness blocks were placed downwind from the spires to adjust the wind velocity profile. The length of the sides of the roughness blocks can be calculated using the following equation (Irwin, 1981).

$$\frac{k}{\delta} = \exp\{\frac{2}{3}\ln(\frac{D}{\delta}) - 0.1161[(\frac{2}{C_f}) + 2.05]^{1/2}\} \tag{8}$$

$$C_f = 0.136\left(\frac{a}{1+a}\right)^2 \tag{9}$$

Here, k represents the length of the sides of the roughness blocks (m), and D represents the spacing between the blocks (in this research, set to a value of 0.05 m). Based on the results of the calculation, the length of the sides of the roughness blocks k was set to 0.01 m.

By using both spires and roughness blocks, it is possible to create a wind velocity profile in the vertical direction (or in other words, to generate a boundary layer) and it is possible to create a constant wind velocity profile in the horizontal direction. In this way, wind tunnels can be improved so that it is possible to perform sand drift experiments even with short settling chambers. An image of the installation of the spires and roughness blocks downwind is shown in Figure 3.9.

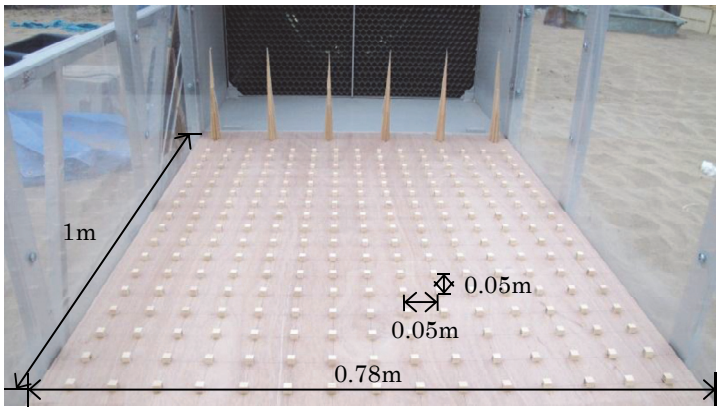

Fig 2.9 Schematic of installation of spire and roughness block

3.4 Results and discussion

Figure 3.10a shows the results of a measurement of the wind velocity in the vertical direction for the condition in which turbulence generators (in other words, spires and roughness blocks) were not used. The boundary layer thickness is determined from a logarithmic approximation using the observation points from the ground to the point where the wind velocity ceases to increase with height. As a result, the thickness of the boundary layer was determined to be 14 cm, which is fairly thin. Examining the wind velocity profile in the horizontal direction (Figure 3.10b) reveals that the wind velocity in the area that is between 20 cm and 60 cm is not affected by the wall. In addition, the standard deviation of the wind velocity profile in the horizontal direction (between 20 cm and 60 cm) is 0.12 m/s, which indicates that the turbulence was relatively large.

Next, Figure 3.11a shows the results of the measurement of the vertical profile of the wind velocity for the condition in which only the spires were used. The thickness of the boundary layer increased by 4 cm, which is a small amount (18 cm). The deviation from the line showing the logarithm approximation decreased greatly compared to the case in which spires were not used. In the horizontal direction (Figure 3.11b), using the spires caused the standard deviation of the wind velocity profile in the horizontal direction to increase (0.17 m/s). These results imply that using spires alone enables the wind velocity profile in the vertical direction to be adjusted somewhat, but also disturbs the wind velocity profile in the horizontal direction.

Next, Figure 3.12a shows the results of the measurement of the vertical profile of the wind velocity for the condition in which both the spires and the roughness blocks were used. The spacing of the roughness blocks in Figure 3 was 5 cm. This value is the initial value for the spacing, but it is also possible to adjust this value based on the results. As a result, the thickness of the boundary layer increased by 20 cm (38 cm). By using the roughness blocks, it is possible to generate a boundary layer that can withstand the sand drift experiments. In the horizontal direction, the standard deviation of the wind velocity profile in the horizontal direction was not very different from the case in which only spires were used (0.19 m/s) (Figure 3.12b). However, the wind velocity profile differs from the profile shown in Figure 5b in that the wind velocity profile in the horizontal direction has been made uniform at intervals of approximately 5 cm due to the effect of setting the spacing between the blocks to 5 cm. Comparing the roughness lengths

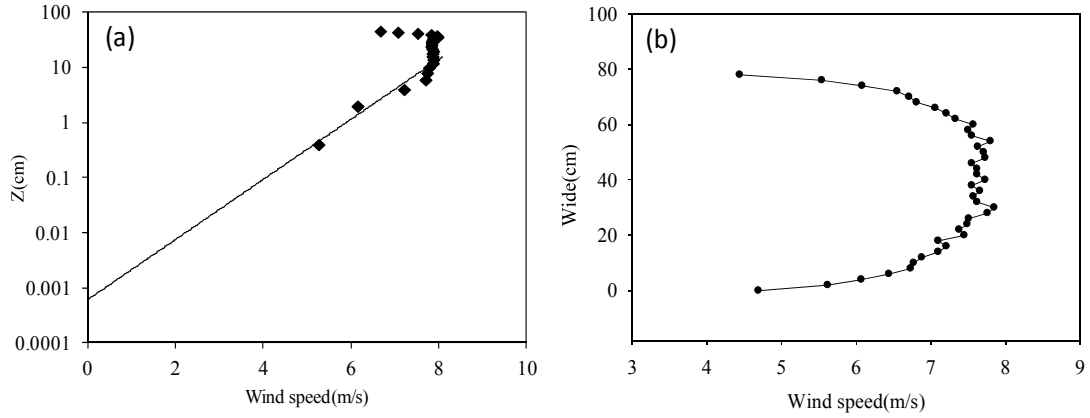

Fig 3.10 Wind velocity distribution in the vertical direction when only the honeycomb is installed (a) and wind speed distribution in the horizontal direction (b)

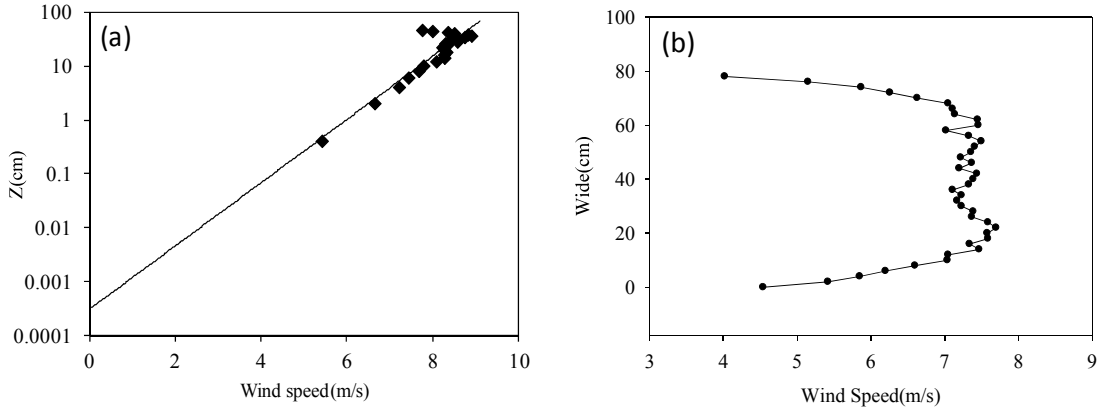

Fig 3.11 Distribution of wind velocity in the vertical direction when spire is installed (a) and wind speed distribution in the horizontal direction (b)

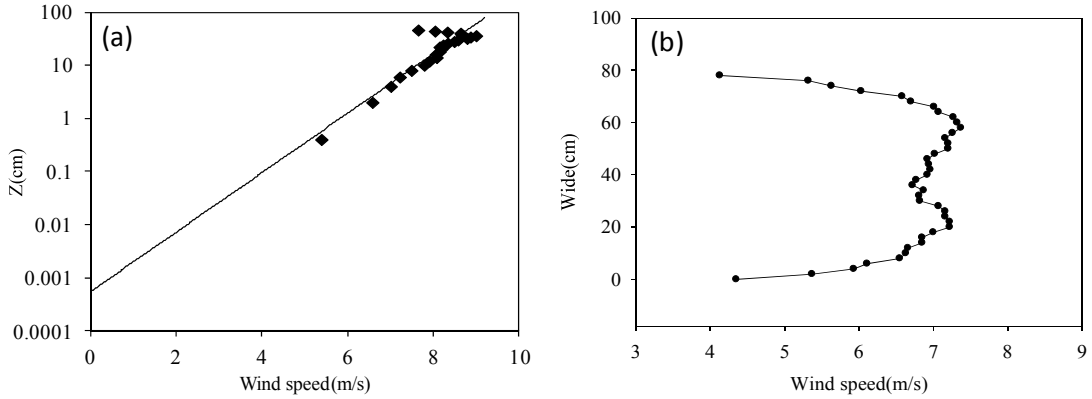

Fig 3.12 Distribution of wind velocity in the vertical direction when spire and roughness block are used together (a) and wind speed distribution in the horizontal direction (b)

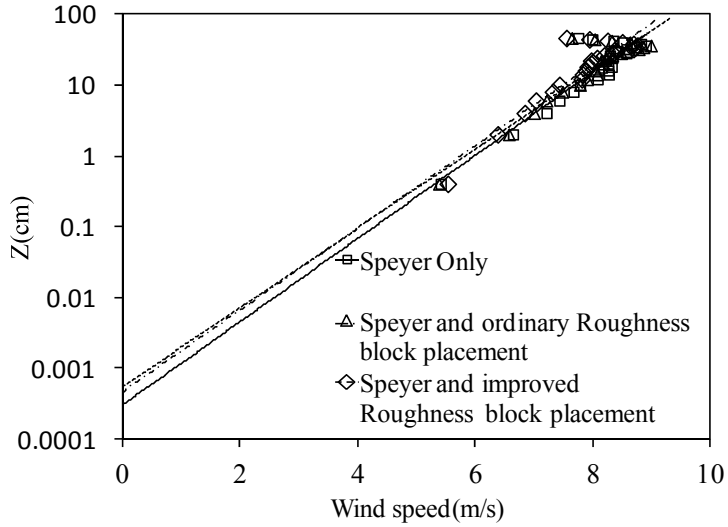

Fig 3.13 Comparison of wind speed distribution and roughness length in the vertical direction with and without roughness block

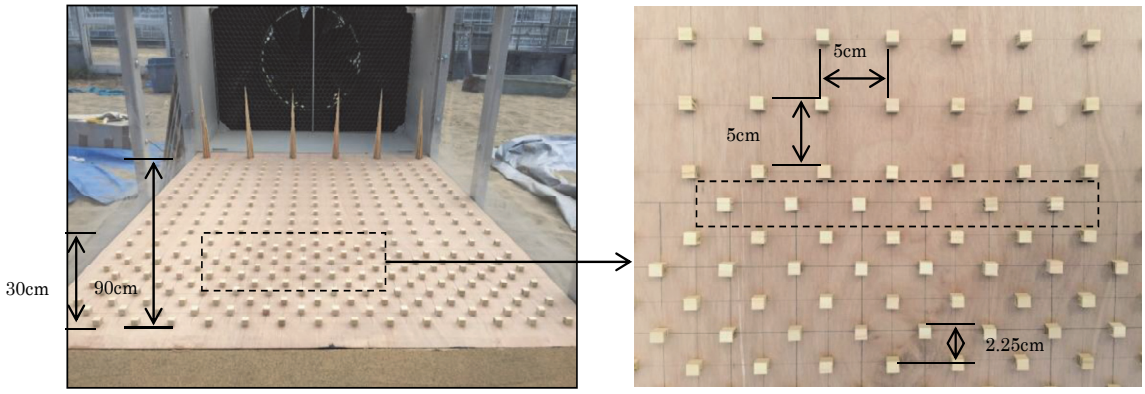

Fig 3.14 Appearance of roughness block devised newly

between the case in which roughness blocks were used and the case in which roughness blocks were not used (Figure 3.13), it can be seen that the roughness length (y-intercept) at the downwind side of the test section was slightly larger when roughness blocks were used, although the difference was not very large. Considering the fact that the roughness length of flat bare land in the natural environment is 1 order of magnitude larger (0.01 cm: Kondo, 1994), this difference is small.

Since the change in the wind velocity profile in the horizontal direction is still large, we investigated and proposed a method for improving the arrangement of the roughness blocks. This method involves combining spires with roughness blocks arranged in two different arrangement densities in order to adjust the wind velocity profile of the

boundary layer in the vertical direction while adjusting the wind velocity profile in the horizontal direction with the roughness blocks.

The idea proposed for the roughness block arrangement densities is shown in Figure 3.14. In the arrangement density proposed in this research (Figure 3.14), the arrangement density in the length direction was increased in order to make the sizes of the turbulence vortices smaller and to make the wind velocity profile in the horizontal

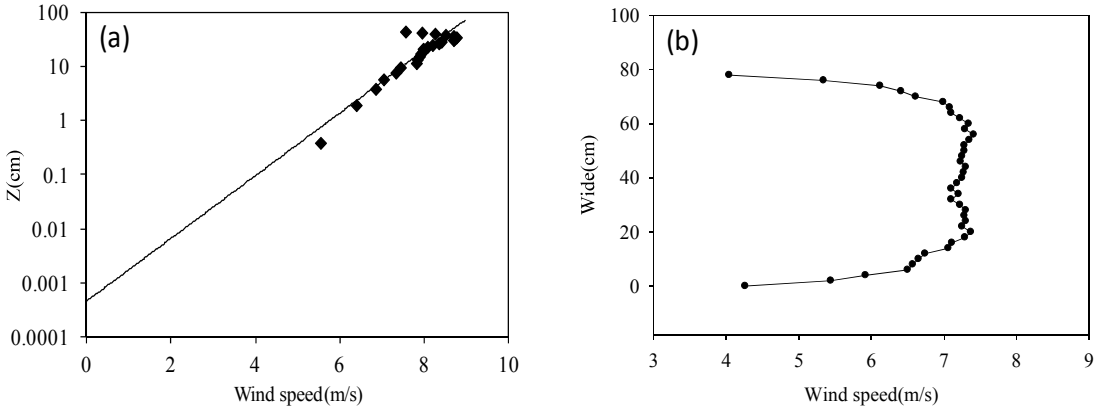

Fig 3.15 Wind velocity distribution in the vertical direction when roughness block arrangement density is changed (a) and Wind speed distribution in the horizontal direction (b)

direction approximately uniform. The results show that although the thickness of the boundary layer did not change (38 cm) (Figure 3.15a), the standard deviation of the horizontal wind velocity profile became 0.08 m/s (Figure 3.15b), which implies that the horizontal wind velocity profile was made approximately uniform. It is anticipated that fine-tuning the spacing of the roughness blocks will result in further improvement of the horizontal wind velocity profile. However, since the accuracy of the profile that was obtained in this experiment was already sufficient (much smaller than the measurement precision of the pitot tube (0.25 m/s)), no further investigation was conducted as part of this research.

3.5 Conclusion

In this research, a method for generating a boundary layer in a small-scale simple wind tunnel using both spires and roughness blocks was proposed. In addition, a method for adjusting the wind velocity profile in the horizontal direction to make it uniform as well as forming a boundary layer was also proposed. The method resulted in a boundary layer with a thickness of 38 cm in a settling distance of 3.6 m. In addition, it was possible to make the wind velocity profile approximately uniform in the horizontal direction by adjusting the arrangement of the roughness blocks. By using spires and roughness blocks together in this way, it is possible to design low-cost small-scale simple wind tunnels with short settling distances. In this research, the dimensions of the wind tunnel were designed beforehand based on estimates for the thickness of the boundary layer required for measurements. The thickness of the boundary layer was further adjusted after completion of the wind tunnel.

In the future, we plan to use this wind tunnel for environmental experiments such as studying wind ripples, sand saltation, mechanisms of yellow dust generation, and countermeasures for yellow dust.

4 A method to make a boundary layer with roughness length

4.1 Introduction

In order to observe sand drift phenomena using wind tunnels, it is important to ensure that experiments are not affected by measurement conditions such as irregular changes in the wind direction and wind velocity (Arien, 1978). Furthermore, it is important to be able to recreate conditions that are similar to the conditions of the natural environment while being able to freely set the experiment parameters. In particular, two conditions that are necessary for wind tunnel experiments include the boundary layer and roughness length, which affect the vertical distribution of the amount of sand drift, and a stable wind velocity profile in the test section.

Liu and Kimura (2016) used devices for controlling the turbulence of the wind spires and roughness blocks) and proposed a method for achieving a flow that has properties that are similar to the atmospheric boundary layer within relatively short settling distances. As a result, the researchers were able to obtain a boundary layer of a thickness of 38 cm within a short settling distance of 3.6 m. Furthermore, by adjusting the arrangement of the roughness blocks, the researchers were able to make the wind velocity in the test section approximately uniform in the horizontal direction. However, the roughness length in the test section was 0.001 cm, which is small. This value is one order of magnitude smaller than the roughness length of flat bare land in the natural environment (for example, 0.01 cm; Kondo, 1994).

In order to use spires and roughness blocks to achieve this roughness length, it is necessary to adjust the resistance to the wind in the settling chamber. In general, the roughness length can be adjusted by changing the sizes of the roughness blocks, the horizontal and vertical spacing of the roughness blocks, and the number of columns（Sill,1988；Yi and Tian,2013）. However, previous research does not provide any methods or procedures for simultaneously achieving roughness lengths that are close to the value found in a natural environment, wind velocity profiles that are constant in the

horizontal direction, and stable wind velocities within the test chamber while maintaining the thickness of the boundary layer at a stable value. The goal of this research is to propose a method/procedure for satisfying these conditions simultaneously using turbulence control devices (spires and roughness blocks) based on the simple small-scale wind tunnel described in Liu and Kimura (2016).

4.2 Overview of simple wind turbine and wind velocity measurement method

The wind tunnel used in this experiment is a single-circuit open-return wind tunnel and is capable of generating a boundary layer (Liu and Kimura, 2016). The wind sent from the fan (maximum output 1.5 kW) passes through the honeycomb that has been installed to straighten the flow. After a turbulent flow is formed in the settling chamber of nominal dimensions 3.6 m × 0.8 m × 0.5 m, a boundary layer with a thickness of 0.38 m can be formed in the test section of dimensions 1.8 m × 0.8 m × 0.5 m. A diagram and a photograph of the wind tunnel are shown in Figure 3.1. The fan is equipped with an inverter, so the wind velocity produced by the fan can be freely set according to the requirements of the measurement (0 m/s–12 m/s).

For measuring the wind velocity, the mainstream wind velocity was set to a constant value of 8 m/s, identical to the method in Liu and Kimura (2016). Moving observations of the wind velocity in the vertical direction and horizontal direction were taken on the upwind side of test section using a pitot tube flow velocity/flow rate micro differential pressure gauge (MK Scientific, Inc.: DT-8920) that was fixed to a stand. The measurement axes in the vertical direction and the horizontal direction were aligned along the height (0.5 m) and width (0.78 m) of the wind tunnel. Measurements were taken at measurement intervals of 0.02 m. The measurement axis for the vertical direction was chosen to be at the center of the upwind side of the test section. The wind velocity profile in the horizontal direction was measured at a height of 4 cm from the floor of the test section. The data was recorded at an interval of 1 second. 1 minute of data was averaged and used for the analysis. In order to measure the wind velocity profile in the vertical and horizontal directions for the case in which the ground is covered in sand, the measurement was taken with a wooden board with sand stuck onto it (fixed to the surface of the wooden board with adhesive) placed on the floor from the settling chamber to the test section.

4.3 Proposal for method which simultaneously achieves roughness length, boundary layer thickness, uniform wind velocity profile in the horizontal direction, and test section with stable wind velocity

4.3.1 Roughness length adjustment method

According to the results presented by Sill (1988), there are two methods for increasing the roughness length using only roughness blocks: ① Increasing the number of vertical columns without changing the size of the roughness blocks and the spacings of the roughness blocks in the horizontal and vertical directions (horizontal and vertical lengths with respect to the wind direction on the surface on which the roughness blocks are laid: Refer to Figure 4.2), and ② changing the size of the roughness blocks and the spacings of the roughness blocks in the horizontal and vertical directions without changing the number of columns. In method ①, it is possible to adjust the roughness length to a certain extent just by increasing the number of columns. However, increasing the number of columns makes it necessary to increase the length of the settling chamber (Yi and Tian, 2013). Therefore, this method is not a realistic option for designing a wind tunnel with a short settling chamber, which is the goal of this research. In method ②, the effect of the roughness blocks extends to an area that is only 5 times the height of the roughness blocks (Sill, 1988). In other words, since the roughness blocks mainly adjust the lower layers of the boundary layer, in order to adjust the upper layers of the boundary layer, it is necessary to set the sizes of the roughness blocks to be complex. For example, using roughness blocks of different heights at the same time enables the vertical profile of the wind velocity to be adjusted. However, one shortcoming of this method is that it requires a large amount of trial and error and much time.

Liu and Kimura (2016) proposed a method for generating boundary layers that are required for performing sand drift experiments using spires and roughness blocks together. The functions of the spires and roughness blocks are shown in Table 4.1. The results show that the spires and roughness blocks provide resistance to the wind sent from the fan, and are helpful in generating boundary layers that are relatively thick. However, the wind velocity profile in the vertical direction is affected by the spires

more than the roughness blocks (Table 4.1). Therefore, we focused on the wind-receiving area of the spire, and hypothesized that minute changes in the wind-receiving area can have an effect on the wind velocity profile in the vertical direction and on the upper layers of the boundary layer in particular. In this research, we propose a method for generating boundary layers that accompany roughness lengths that are similar to those found in natural environments by adjusting the shape of the spires.

Table 4.1 Role of spiers and roughness blocks

Role of speyer	Role of roughness block
Adjustment of boundary layer thickness (Particularly in the upper part)	Adjustment of boundary layer thickness (Particularly in the lower part)
Vertical wind speed distribution	Fine adjustment of wind speed distribution in the vertical direction
	Horizontal wind speed equality

4.3.2 Adjustment of spire shape

The height (0.23 m) and width (bottom side of the triangle of the bottom face: 0.024 m) of the spire were chosen based on the research presented by Liu and Kimura (2016) and Irwin (1981). In order to increase the wind-receiving area of the spires without changing their height or width, we considered increasing the width of the top end of the spires. This change caused the shape of the wind receiving face of the spires to change from a triangle shape to a trapezoidal shape (hereafter, we refer to these spires as trapezoidal spires). The width of the top end of the trapezoidal spires was chosen to be 0.003 m, based on the results presented by Ham and Bogusz (1998) (Figure 4.1a). Similar to Liu and Kimura (2016), 6 spires were lined up horizontally with a spacing of 0.125 m (Figure 4.1b). In order to increase the resistance to the wind, the material used for the spires was changed from wood to acrylic board with a thickness of 0.05 m. The roughness blocks (height 0.1 m, width 0.09 m) were arranged with a spacing of 5 cm in an area of length 0.55 m and width 0.6 m, similar to the arrangement used by Liu and Kimura (2016). Furthermore, additional roughness blocks were paced downwind with an increased density with a spacing of 2.5 cm in an area of length 0.25 m and width 0.5 m (indicated by numbers in Figure 4.2).

In this research, we hypothesized that trapezoidal spires and roughness blocks can be used together to generate boundary layers that are relatively thick and have roughness lengths that are similar to those of the natural environment while maintaining the uniformity of the wind velocity profile in the horizontal direction and maintaining the stability of the wind direction and wind velocity in the test section. Figure 4.2 shows a photo of how the trapezoidal spires and roughness blocks are installed.

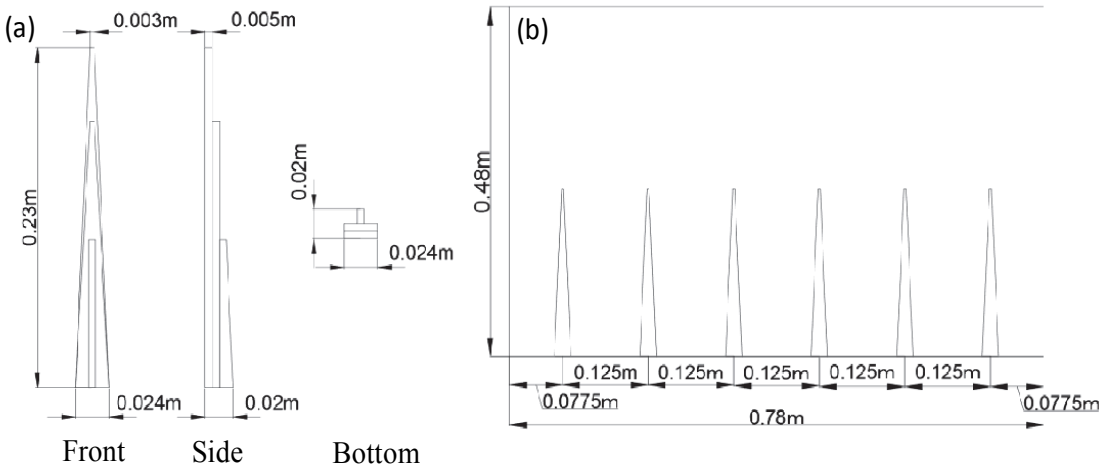

Fig 4.1 Trapezoid spire specification (a) and installation overview (b)

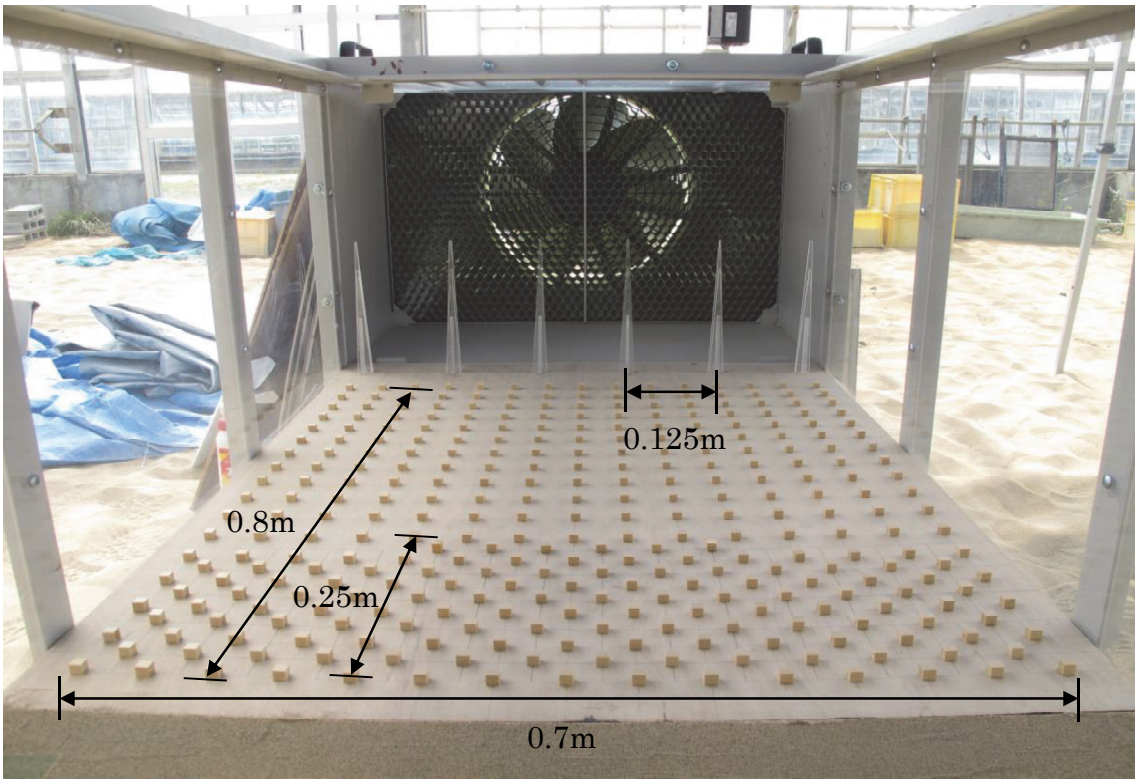

Fig 4.2 Overview of installation of trapezoid spears and roughness blocks in the rectification field

4.4 Results and discussion

4.4.1 Generation of a boundary layer with roughness length that is similar to that of the natural environment

Figure 4.3a shows the results of a measurement of the wind velocity profile (in the vertical direction) for the condition in which both trapezoidal spires and roughness blocks were used. The thickness of the boundary layer was 0.34 m. This result is almost identical to the result of Liu and Kimura (2016). However, the roughness length increased by one order of magnitude and became approximately 0.01 cm. Making the

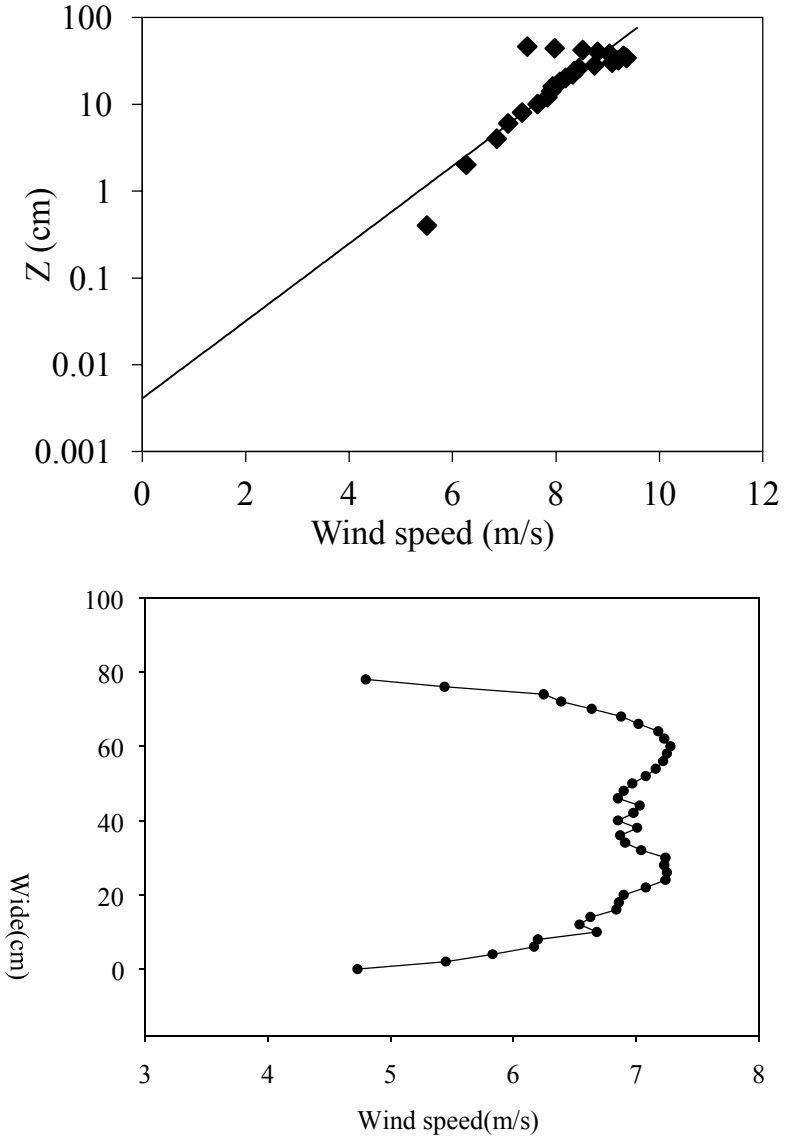

Figure 4.3 Vertical wind speed distribution (a) and horizontal wind speed distribution (b) when trapezoid spear and roughness block are used in

wind-receiving face of the spires trapezoidal in shape enabled us to generate a boundary layer that was relatively thick and increase the roughness length at the same time. However, the variation in the wind velocity profile in the horizontal direction (taken at a height of 4 cm and width of 20 cm to 60 cm away from the wall) was large. The standard deviation of the difference of the wind velocity was 0.15 m/s (Figure 4.3b). Compared to the results presented by Liu and Kimura (2016), the variation increased by a factor of 2.

Therefore, in order to make the wind velocity profile in the horizontal direction more uniform, we tried changing the arrangement of the roughness blocks downwind. Since changing the arrangement of the blocks would require a large amount of time for measurement, wind velocity data was taken only in the range from 20 cm to 60 cm away from the wall for measuring the wind velocity profile in the horizontal direction. The difference in the wind velocity profiles in the horizontal direction caused by the difference in the arrangement of the blocks is shown in Figure 4.4. In case a, 20 roughness blocks were added with a spacing of 2.5 cm over an area of vertical width 0.1 m and horizontal width 0.5 m. As a result, the standard deviation of the difference in the wind velocity in the horizontal direction became 0.33 m/s. In case b, 40 roughness blocks were added with a spacing of 2.5 cm over an area of vertical width 0.2 m and horizontal width 0.2 m on the side of the left wall, and over an area of vertical width 0.2 m and horizontal width 0.3 on the side of the right wall (the resulting standard deviation was 0.27 m/s). In case c, 46 roughness blocks were added with a spacing of 2.5 cm over an area of vertical width 0.2 m and horizontal width 0.6 m (the resulting standard deviation was 0.28 m/s). In case d, 102 roughness blocks were added with a spacing of 2.5 cm over an area of vertical width 0.35 m and horizontal width 0.6 m (the resulting standard deviation was 0.26 m/s).

Examining the results shown in Figure 4.4 shows that the wind velocity profiles in cases a, c, and d have only a narrow range in which the wind velocity is uniform. On the other hand, although the value of the standard deviation of the difference in wind velocity shown in case b is no different (compared to the other cases), the range in which the wind velocity is uniform is large. However, the value of the standard deviation of the difference of the wind velocity did not improve compared to its value

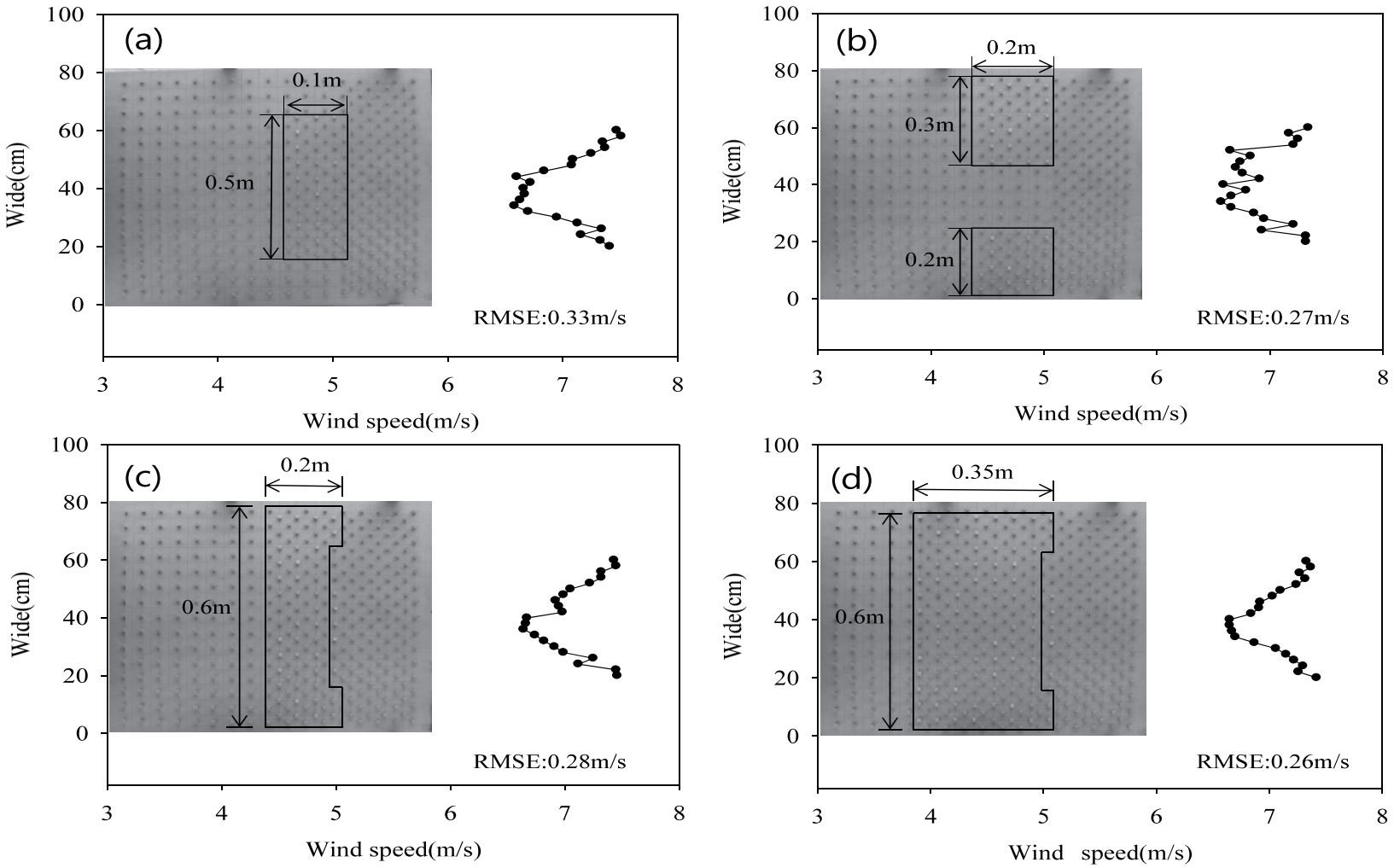

Fig 4.4 Relationship between roughness block arrangement method and horizontal wind speed distribution

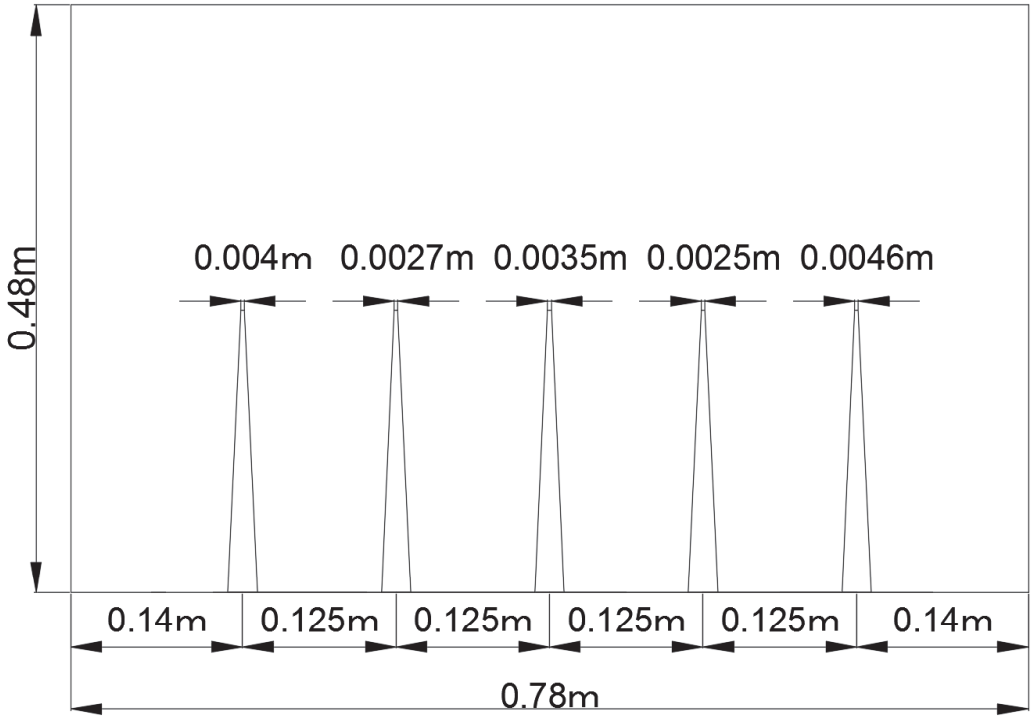

Fig 4.5 New arrangement of trapezoid spire

before the arrangement of the roughness blocks was changed (0.15 m/s). In other words, these results indicate that changing the arrangement of the roughness blocks does not have a large impact on the uniformity of the wind velocity profile in the horizontal direction.

Therefore, we shifted focus to the spires again. We hypothesized that it is possible to decrease the turbulence intensity without affecting the shape of the boundary layer, or in other words to make the wind velocity profile in the horizontal direction become uniform, by decreasing the area of the wind tunnel cross-section that captures the wind without changing the slope angle of the spires (angle between the diagonal side and bottom side). In order to validate this hypothesis, we decreased the number of spires from 6 to 5 without changing the spacing (Figure 4.5). The roughness blocks were arranged in the same way as was done by Liu and Kimura (2016). The wind velocity profile in the vertical direction is shown in Figure 4.6a. The thickness of the boundary layer was 38 cm. Although the standard deviation of the difference of the wind velocity in the horizontal direction decreased to 0.09 m/s (Figure 4.6b), the range in which the wind velocity is approximately constant is biased to one side (26 cm - 68 cm), and the

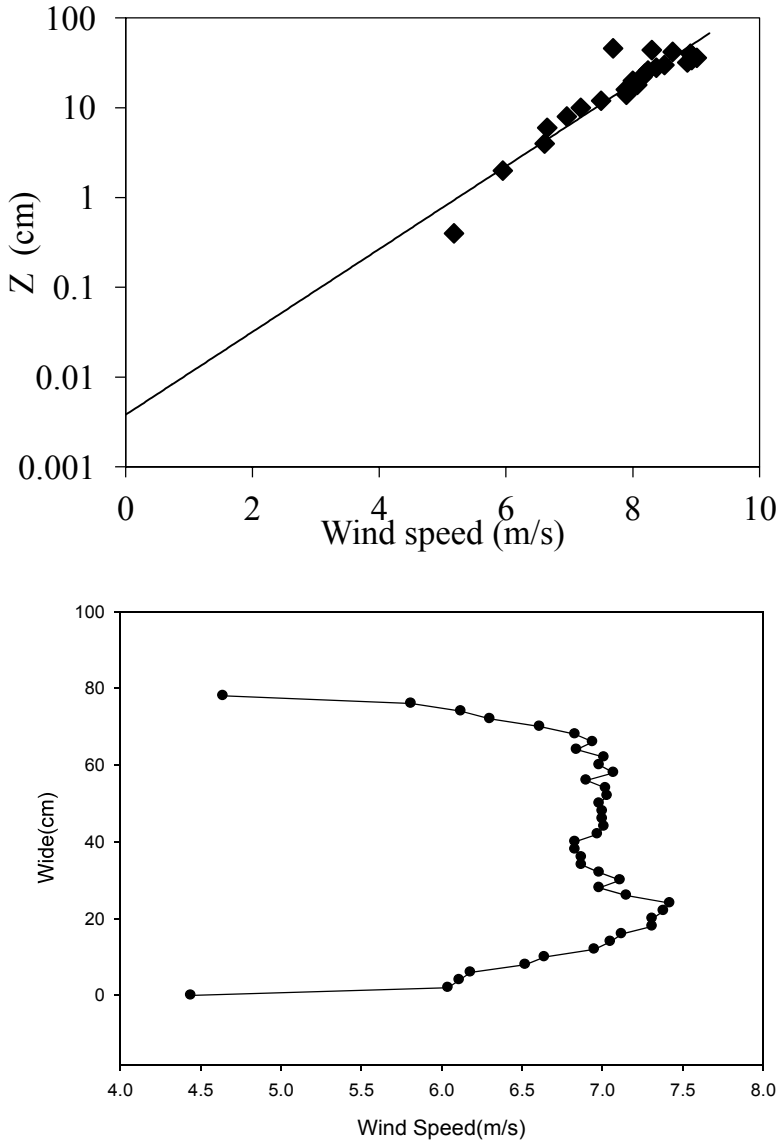

Fig 4.6 Vertical vertical wind speed distribution (a) and horizontal wind speed distribution (b) when newly devised speyer is placed.

wind velocity still has large variation especially in the range from 16 cm - 20 cm. We tried to identify the cause of the variation in the range from 16 cm - 20 cm. In this research, we designed the trapezoidal spires to have a top end width of 0.003 m. However, the acrylic boards were thick (0.005 m) and difficult to machine with high precision, so we were unable to make their widths strictly uniform (Figure 4.6). In other words, we believe that the reason for the variation in the wind velocity profile in the horizontal direction is the fact that the slope angles of the spires are not uniform.

Therefore, in order to make the widths of the top ends uniform, we changed the thickness of the acrylic boards to 0.003 m, and redesigned the widths of the top ends to be 0.005 m. Since the 0.003 m acrylic boards are thin, there is a chance that vibrations will occur during experiments with high winds. In order to overcome this issue, we installed triangular struts of height 0.15 m to the spires (Figure 4.7). 5 spires were lined up horizontally at a spacing of 0.125 m (Figure 4.8). The roughness blocks were arranged in the same way as was done by Liu and Kimura (2017). As a result, the boundary layer thickness was unchanged at 38 cm. However, the standard deviation of the difference of the wind velocity in the horizontal direction became 0.1 m/s, which is smaller, and the range in which the wind velocity was uniform was not biased (Figure 4.9). In the end, we were able to generate a boundary layer with a roughness length that is close to that found in the natural environment while simultaneously creating a wind velocity profile that is uniform in the horizontal direction without changing the arrangement or density of the roughness blocks and by adjusting only the spires.

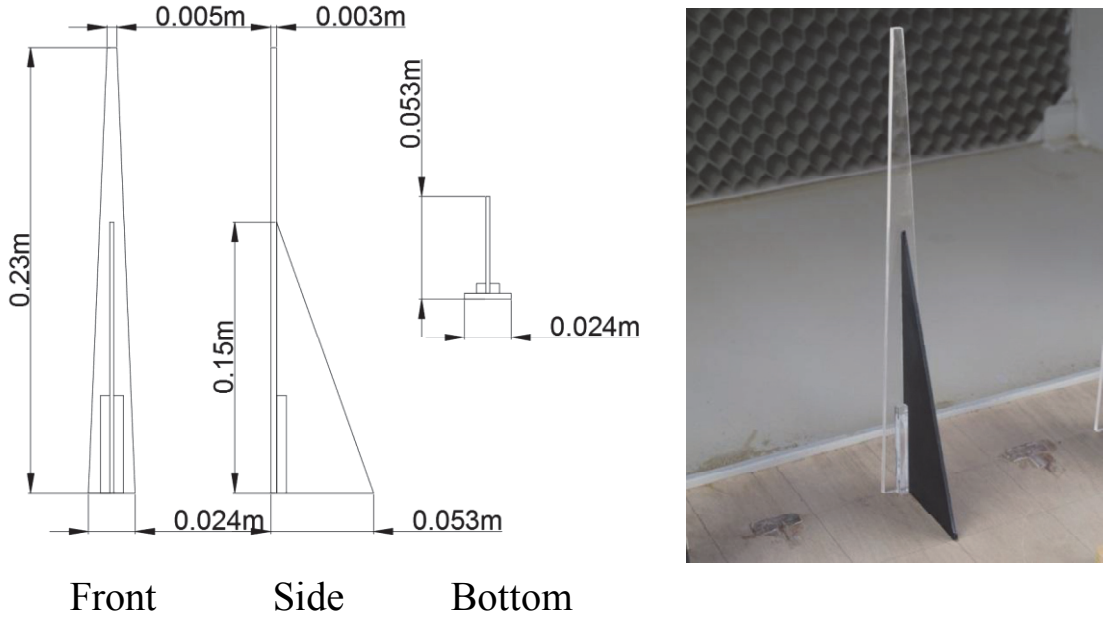

Fig 4.7　New trapezoid spire specification

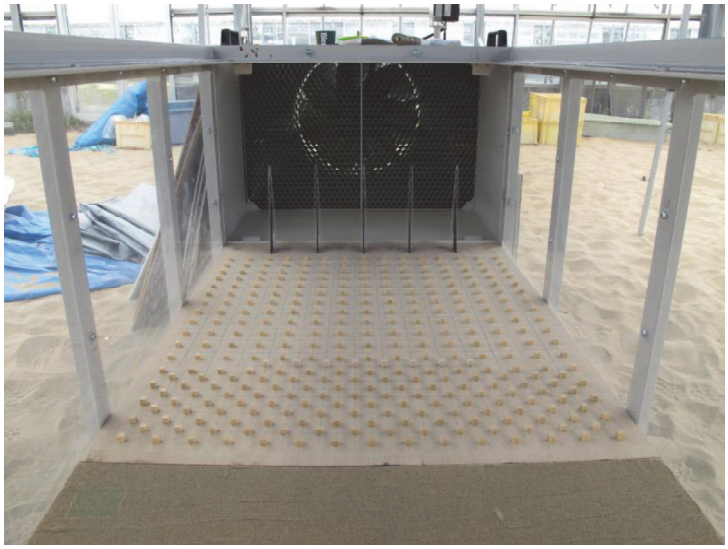

Fig 4.8 Pictures of the turbulence generator installation method

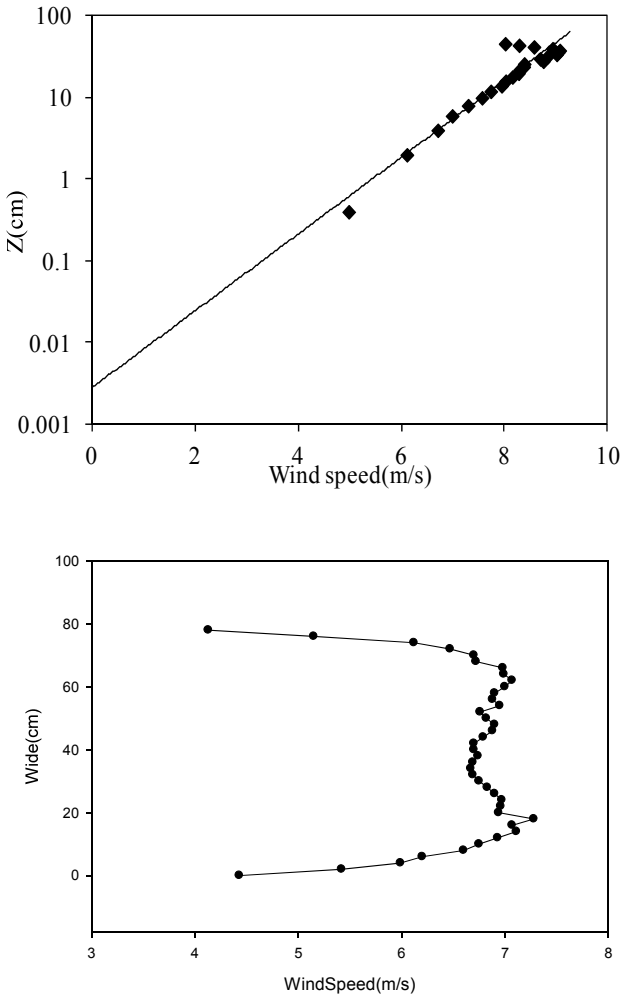

Fig 4.9 Vertical wind speed distribution (a) and horizontal wind speed distribution (b) when new trapezoid spire and roughness block are used together.

4.4.2 Generation of a stable test section

In the measurements and analyses above, the wind velocity was only measured at the entrance of the test section. However, when conducting sand drift experiments in the future, the experiments will be conducted using the entire test section. In this case, it is necessary to control the vertical profiles of the wind velocity at the entrance and exit of the test section to be approximately uniform. Figure 4.10 shows a comparison of the results of measurements of the vertical distribution of the wind velocity in the test section at a spacing of 0.6 m taken at 4 locations. Although the boundary layer width at the upwind side of the test section was 0.38 m, the boundary layer widths that were measured at the 3 locations on the downwind side were all 0.36 m. The results for the wind velocity profiles in the vertical direction were almost identical. In other words, these results imply that the effect of the adjustments made by the spires and roughness blocks on the test section was small.

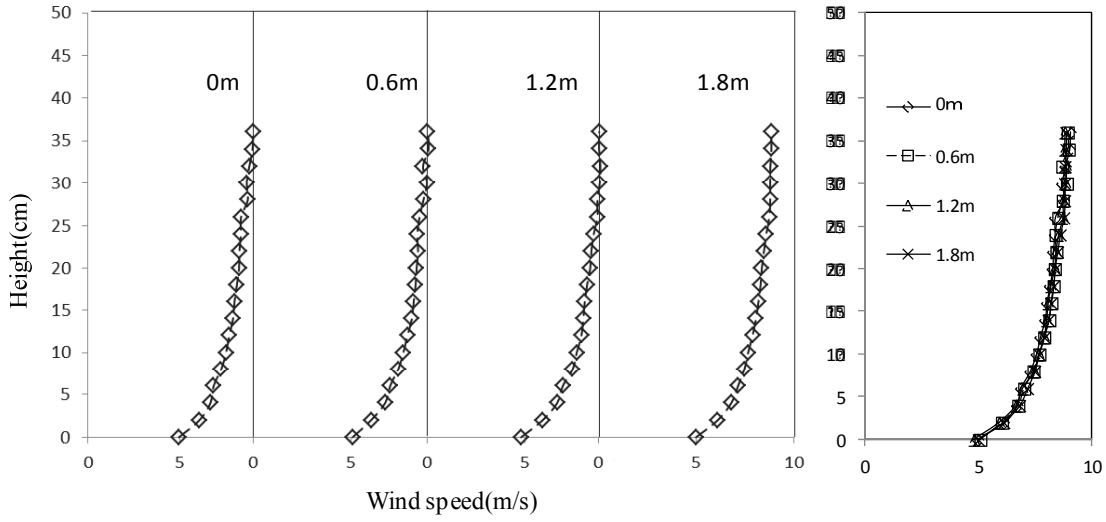

Fig 4.10 Comparison of wind velocity distribution in the vertical direction measured at 4 locations from the upper wind end to the lower wind end of the observatory

4.5 Conclusion

In this research, we proposed a method/procedure for simultaneously generating boundary layers that are relatively thick and have roughness lengths that are similar to those found in the natural environment, creating wind velocity profiles that are uniform in the horizontal direction, and creating wind velocities that are stable in the test section by using turbulence control devices (spires and roughness blocks) based on the simple small-scale wind tunnel described in Liu and Kimura (2016). The results show that it is possible to achieve these goals without changing the arrangement or density of the roughness blocks and by adjusting the shape and number of trapezoidal spires.

Specifically, first we set the height sand bottom end widths of the trapezoidal spires and roughness blocks using the empirical formulas determined by Irwin (1981). Next, we modified the heights of the trapezoidal spires and widths of the bottom ends in order to adjust the upper layers of the boundary layer. We obtained the desired boundary layer width and roughness length. For adjusting the lower layers of the boundary layer, we modified the arrangement density of the roughness blocks and the number of trapezoidal spires to obtain a wind velocity profile that is uniform in the horizontal direction.

In the future, we plan to use this method for adjusting wind flow in simple wind tunnels proposed in this research to achieve conditions that are necessary for conducting sand drift experiments. We anticipate that this will help researchers conducting research for understanding the mechanisms of sand drift occurrence and developing mechanisms for suppressing sand drift.

5 Wind speed characteristics and blown sand flux of gravel surface

5.1 Introduction

The variation of wind speed with the height is called the wind speed protile. Even in similar wind speed conditions, the wind speed vertical gradient changes depending on the state of the ground surface. Under smooth ground surface conditions, the change in the wind speed with height follows logarithmic law, but if the ground surface has gravel, the logarithmic law within a specific height is destroyed. Therefore, the influence of the roughness of ground surface on the boundary layer has become a big problem. In recent years, studies investigating the hydrodynamic characteristics of blown sand in the ground boundary layer using large gravel or mixed type gravel are increasing. However, sufficient knowledge about the characteristics of wind speed protile and the blown sand flux due to the arrangement density of gravel has not yet been obtained. In particular, an experimental method to quantitatively evaluate the distribution of blown sand flux, using a wind tunnel that implements a flow having characteristics close to the atmospheric boundary layer, is desired. Currently, most of the methods for measuring blown sand flux use trap-type sand trapping devices. However, due to reasons such as 1) difference in the individual trapping efficiencies, 2) time taken to trap a certain amount of sand is very long, 3) possibility of obtaining only the time average data of the blown sand flux and so on, elucidation of the phenomenon has been hindered.

Liu and Kimura (2017) generated a 0.36m boundary layer with a short rectification distance of 3.6m, using a compact wind tunnel and a turbulence generator (spires and roughness blocks). Moreover, the result that the wind speed distribution in the vertical and the horizontal directions are almost the same, has also been obtained within the 1.8m observatory. In this study, by introducing the compact and simple wind tunnel device and a piezoelectric blown sand meter that uses a piezoelectric transducer capable of measuring the time variation of blown sand flux, we compare the influence of the variation of gravel coverage rate on the aerodynamic characteristics and blown sand

flux. In addition, we examine the characteristics of blown sand flux distribution measured using the piezoelectric blown sand meter.

5.2 Outline of the experimental apparatus

The blow-down type wind tunnel used in this experiment consists of a blower, a rectifying space, and an observation space. The total length is 8.25 m and the cross-section is 0.8 m*0.5 m (Figure 3.1). The ceiling and the sides of the rectification space (length: 3.6 m) and the observation space (length: 1.8 m) are made of acrylic with a thickness of 0.08 m. Since an inverter (maximum output: 1.5 kW) is installed, the wind speed can be arbitrarily adjusted within the range of 0 to 12 m/s. Creating a boundary layer with a thickness of 0.36m using spires and roughness blocks in combination (roughness length: 0.01 cm), the wind speed distribution in the horizontal direction can be made uniform with an error of 0.1 m/s. The piezoelectric blown-sand meter uses the piezoelectric transducer used in high-precision ultrasonic sensors and measures the number of sand particles from the voltage signal generated by the sand particles colliding on the piezoelectric transducer. Since a cone-type resonator with a diameter of 0.65 m is mounted on the sensor portion of the piezoelectric transducer, under the conditions with a wind speed of 6 to 11 m/s, the number of blown sand grains can be measured with high accuracy.

5.3 Experimental method

5.3.1 Measurement of wind speed characteristics

When measuring wind speed protile, to prevent the failure of the anemometer (pitot tube type) due to the generation of blown sand, sand-affixed to a wooden board for observation was placed on the floor space from the rectification space to the observation space (4.5 m). The median particle size of sand was 350 μm. The particle size of the gravel used for observation (produced in the Tenryu river basin) was 0.005 to 0.01 m. The gravel coverage rate was set to six patterns, 5%, 10%, 15%, 20%, 25% and 30%. Further, in order to measure the amount of sand deposited, the gravel of each coverage rate was fixed to a sand-affixed wooden board (0.9 m*0.4 m) and the measurement was carried out.

Wind speed was set to three patterns, 6 m/s, 8 m/s and 10 m/s with 6 m/s, the generation speed of blown sand, as the base. For the measurement of wind speed, a Pitot tube type anemometer (Pitot tube type wind speed/wind flux differential pressure gauge DT-8920) was used, which was fixed on a stand that can be fine tuned. The measurement axis of the wind speed distribution in the vertical direction was set to the center of the leeward side of the observation space. The measurement was carried out along the vertical measurement axis in the height range of 0.004 m to 0.46 m (space 0.02 m). The recording time interval of wind speed data was set to 1 s and the average of the instantaneous wind speed data for 60 s was taken as the average wind speed of the location.

The wind speed distribution in the vertical direction, when no blown sand is generated, is given by the following equation (1).

$$u_z = 5.57 u_* log \frac{z}{z_0} \tag{10}$$

Here, u_z is the wind speed at a height z above the sand surface, u_* is the friction velocity and z_0 is the roughness length.

5.3.2 Measurement of blown-sand flux

In order to provide a sufficient amount of sand for the observation of blown sand flux, dunes of sand of about 0.1 m in thickness were spread from the rectification space to the observation space (Height of the wind tunnel cross-section was about 46 cm). Under the five patterns of wind speed conditions (6,7,8,9 and10 m/s), gravels with seven patterns of coverage rates (0,5,10,15,20,25 and 30%) were spread on the wooden board where the sand dune had been affixed and the observation was carried out in the observation space.

Ten pieces of piezoelectric blown sand meters were installed on the leeward side the observation space. The blown sand flux was measured at 10 locations from the sand surface to a height of 0.2 m (interval 0.02 m).

The number of blown sand particles *n* measured by the piezoelectric blown sand meter was converted to blown sand fluxq_{Sensor}, using the following equation (Udo, 2008).

$$q_{Sensor} = \frac{\frac{4}{3}\pi(\frac{d}{2})^3\rho_s}{\pi(\frac{d_{PS}}{2})^2 t_0} n = \frac{2\rho_s d^3 n}{3{d_{PS}}^2 t_0} \quad (11)$$

$$q_{Trap} = 10.571 q_{Sensor} \quad (12)$$

Here, d is the median particle size of sand, ρ_s is the density of sand (2.65 x $10^3 \mathrm{kg/m^3}$), d_{PS} is the diameter of the sensor portion of the blown sand meter (0.012 m) and t_0 is the measurement time (1 s).

5.4 Results and discussion

5.4.1 Wind speed distribution

As an example, the observation results of the vertical distribution of wind speed for the (7 patterns) gravel coverage rate due to the three patterns of wind speed conditions (6, 8, and 10 m/s) are shown in Figure 5.1. The horizontal axis and the vertical axis represent the wind speed and the logarithm of height respectively and a boundary layer of about 0.34 m was present.

The friction velocity was calculated using the logarithmic law of wind speed. At any wind speed, the friction speed increased with the increasing coverage rate when the gravel coverage rate was in the range of 0% to 15%. On the other hand, when the coverage rate was 20% or more, the friction speed became smaller than in the case of 0% to 15%.

Focusing on the roughness length, when the gravel coverage rate was in the range of 0% to 15%, the roughness length increased with an increase in the coverage rate (Figure 5.2, Table 5.1). However, when the density of gravel became 20% or more, the roughness length decreased and approached a value close to a roughness length of 0%. Together with the results of friction speed, it can be considered that when the gravel density became 20% or more, the ground surface became aerodynamically smooth and the resistance to wind decreased.

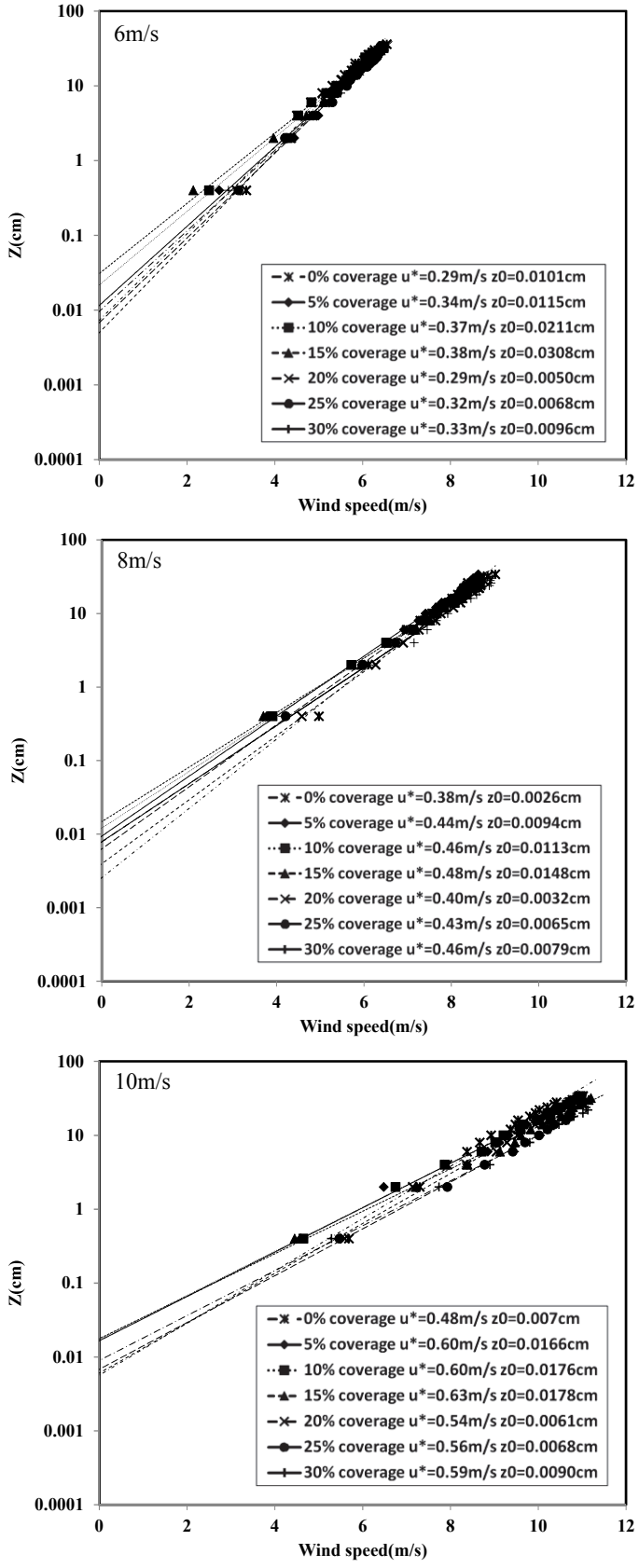

Fig 5.1　Observation results of the vertical distribution of wind speed

Table 5.1 Standard deviation of average roughness length

Cover （%）	Z_0（cm）
0	0.007±0.004
5	0.013 ±0.004
10	0.017 ±0.005
15	0.021±0.009
20	0.005±0.001
25	0.007±0.0001
30	0.009±0.0008

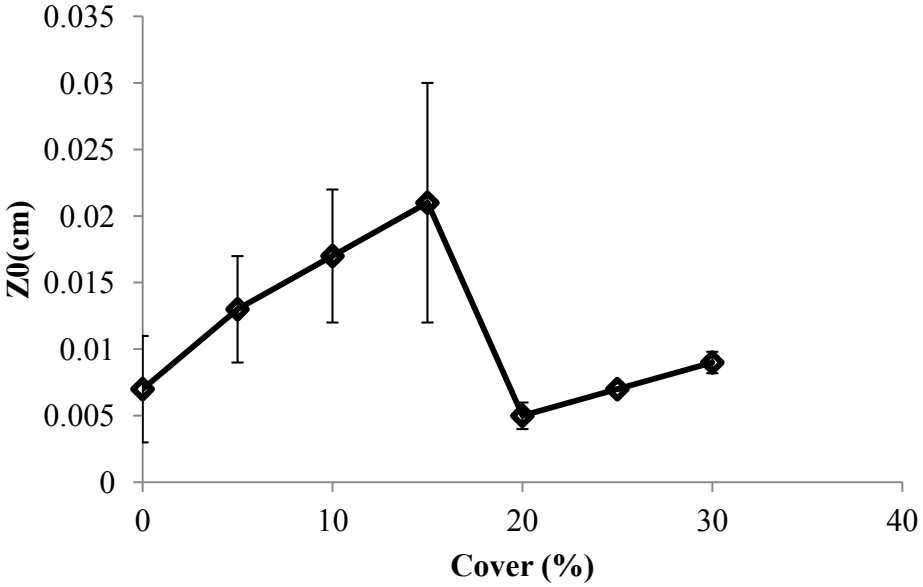

Fig 5.2 Standard deviation of average roughness length

5.4.2 Blown sand flux

We examined the variation in the blown sand flux due to the five patterns of wind speed (6, 7, 8, 9, and 10 m/s), for the seven patterns of gravel coverage rates (Figure 5.3). The horizontal axis shows the height and the vertical axis shows the blown sand flux converted from the number of blown sand particles, n, measured by the piezoelectric blown sand meter.

When the wind speed was 6 m/s, a sand trapping effect was seen within a height of 8 cm for a gravel coverage rate of 5% or more and when the coverage rate became 15% or more, it was completely trapped.

When the wind speed reached 7 m/s, the trapping effect existed up to a gravel coverage rate of 10% at a height of less than 4 cm, but, when the height was 6 cm or more, the effect disappeared. Conversely, at a height of 6cm or more, due to the bound effect of sand particles (Kenneth and Haim, 2009), the blown sand flux increased more than when the coverage rate was 0%. When the coverage rate was 15% or more, the trapping effect was sustained.

When the wind speed reached 8 m/s, the overall trapping effect started to fade. Within a height of 4 cm, as the coverage rate increased, the trapping effect was more. At 8 cm or more, the blown sand flux approached the value at 0% for any coverage rate.

It can be understood that when the wind speed was 9 m/s, the trend was almost similar to the case of 8 m/s, but when the wind speed reached 10 m/s, the effect of blown sand supplementation by the gravel coverage almost disappeared.

Further, it is understood that when the wind speed was 8 m/s or more, the blown sand flux at a height of 8 cm extremely increased when the gravel coverage rate was 20% or more. Figure 5.4 shows the height distribution of the blown sand flux with respect to the change in wind speed for each gravel coverage rate. At any gravel coverage rate, the blown sand flux increased with an increase in wind speed. From the figure, it can be seen that when the gravel coverage rate was 20% or more and the wind speed was 8 m/s or more, the blown sand flux at a height of 8 cm extremely increased.

Figure 6 shows the comparison between the roughness length and the blown sand flux at a height of 8 cm for each coverage rate. Since the gravel coverage rate increased from 0% to 5% due to the bound effect of the blown sand, the blown sand flux increased. However, in the coverage rate range of 5% to 15%, when the wind speed became 8 m/s

or more, the blown sand flux decreased with an increase in the roughness length. On the other hand, when the coverage rate reached 20% and the roughness length approached a value close to that at 0%, the blown sand flux started increasing again and within a range of up to 30%, there was no remarkable variation in the blown sand flux. Therefore, it is implied that when the gravel coverage rate becomes 20% or more, although the total blown sand flux at a height less than 8cm decreases, due to aerodynamic smoothening, the blown sand flux at a height of 8cm alone remarkably increases.

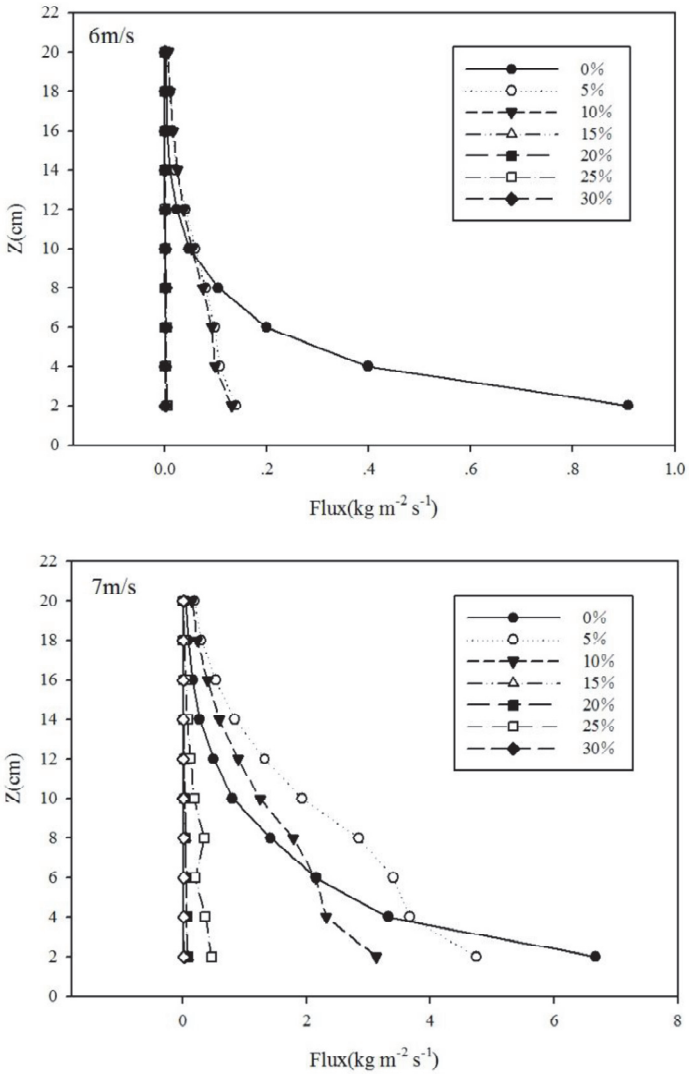

Fig 5.3 Blown sand flux due at wind speeds of 6 m / s and 7 m / s.

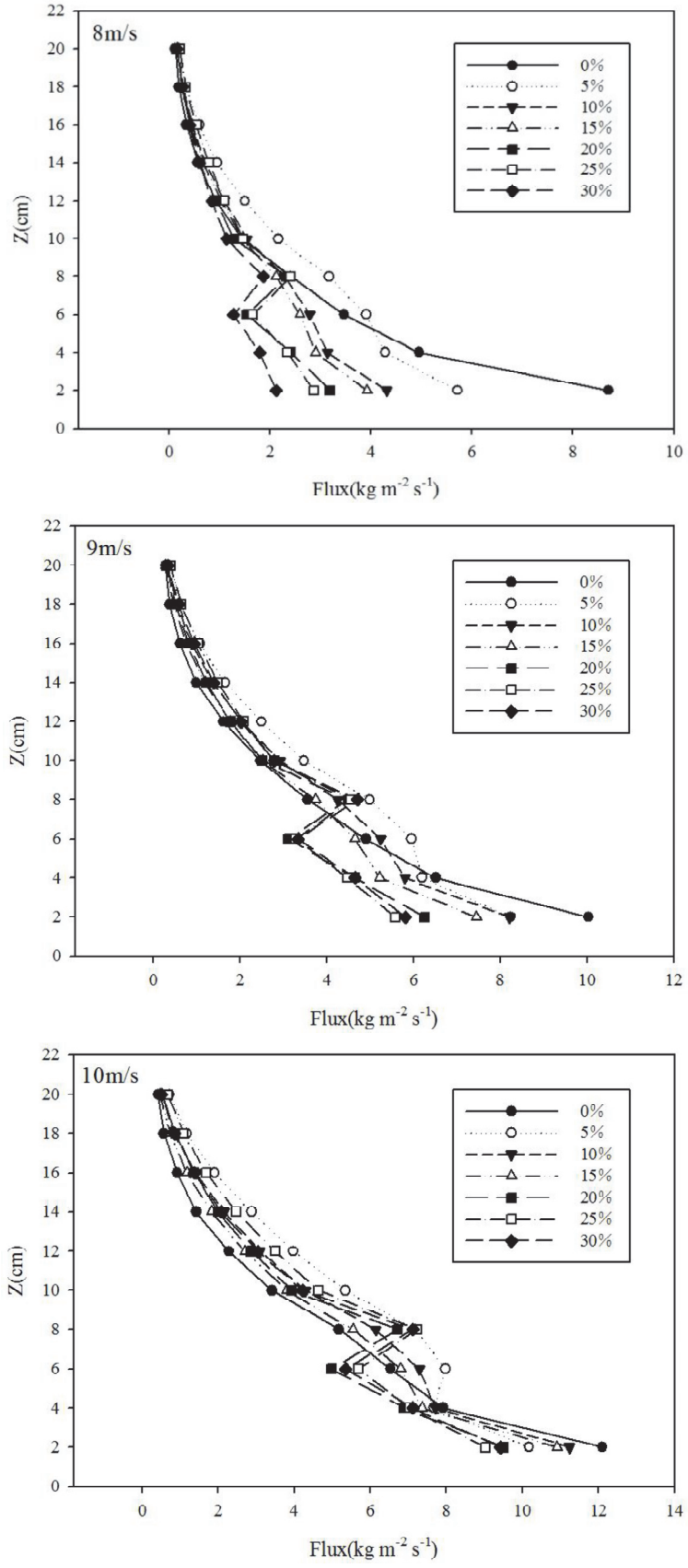

Fig 5.3 Blown sand flux at wind speeds of 8 m / s, 9 m / s, 10m / s.

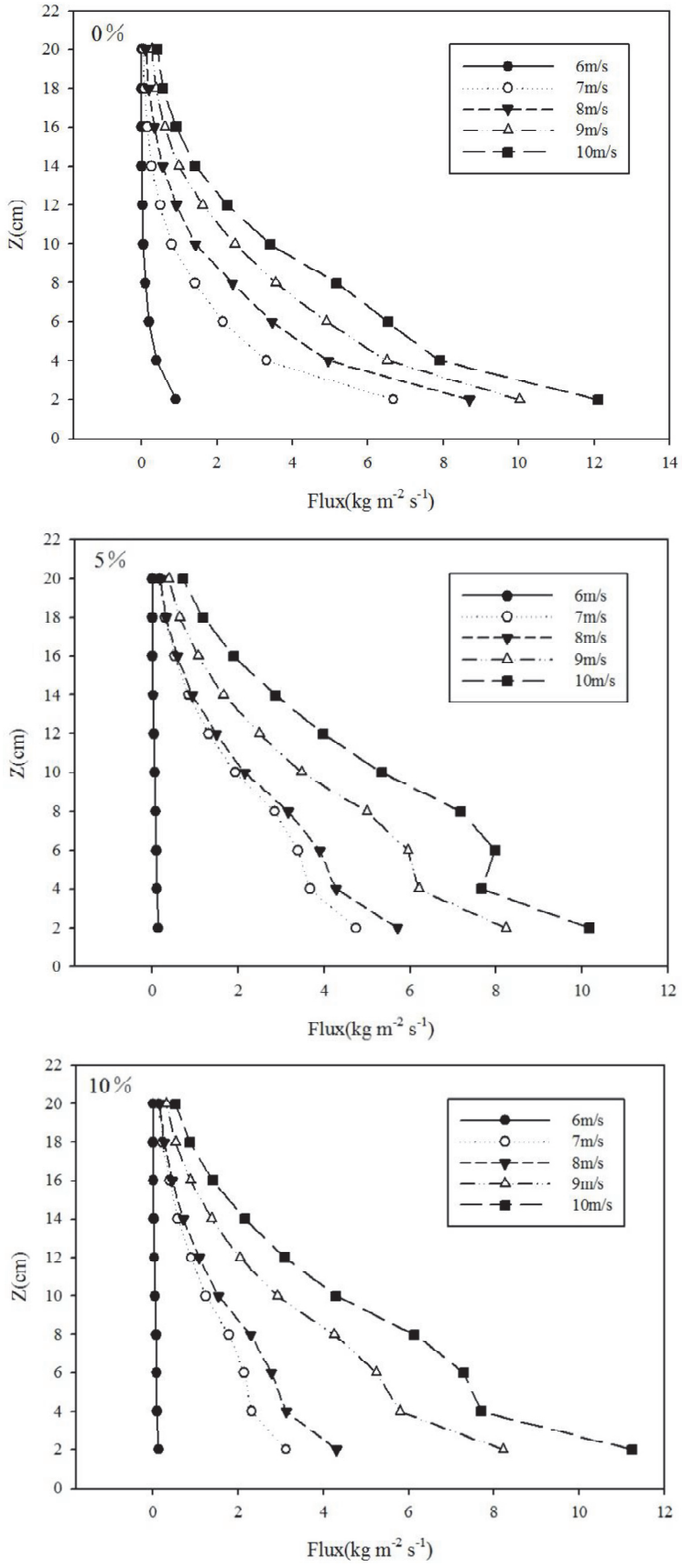

Fig 5.4 Blown sand flux with change in wind speed for each gravel coverage rate.

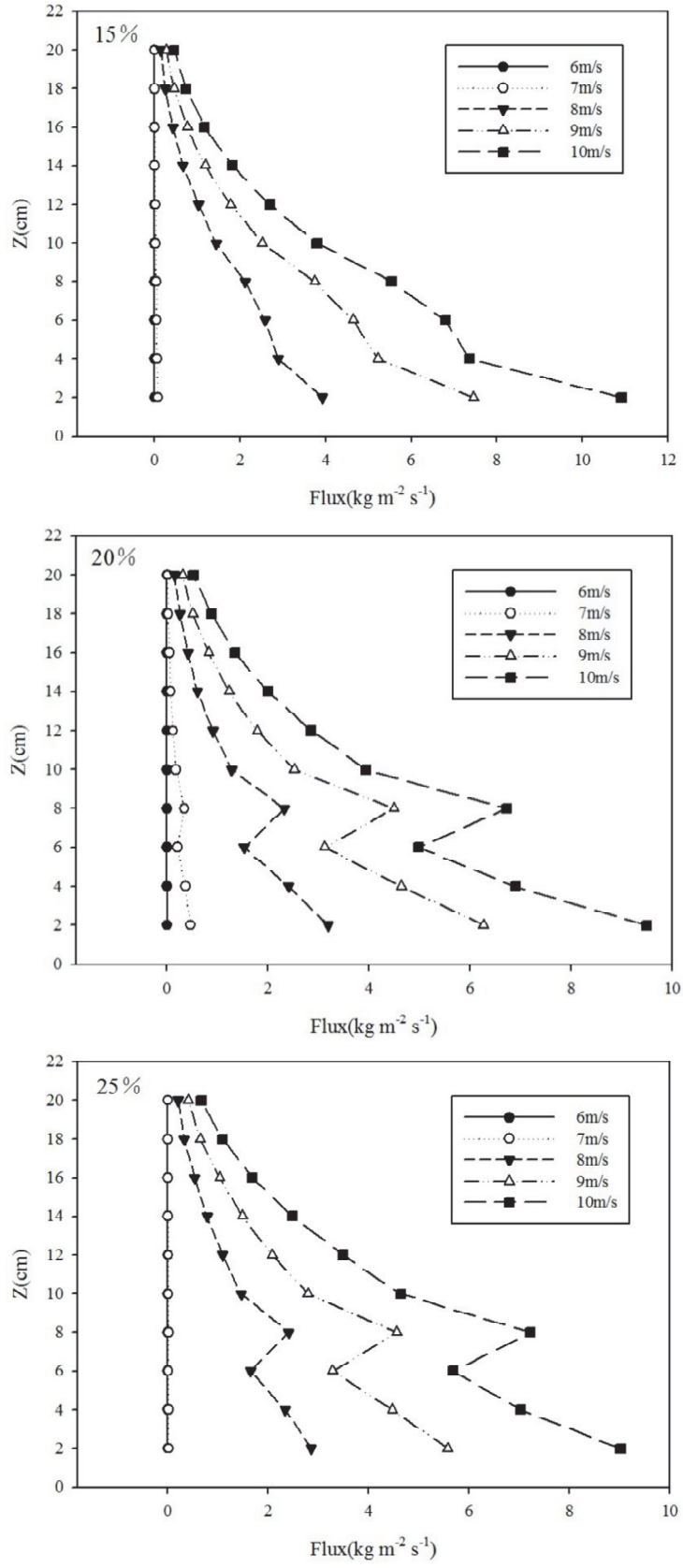

Fig 5.4 Blown sand flux with change in wind speed for each gravel coverage rate.

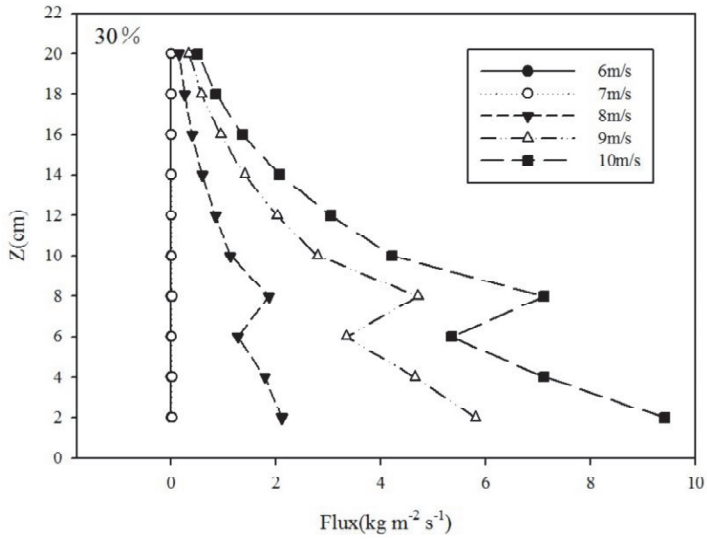

Fig 5.4 Blown sand flux with change in wind speed for each gravel coverage rate.

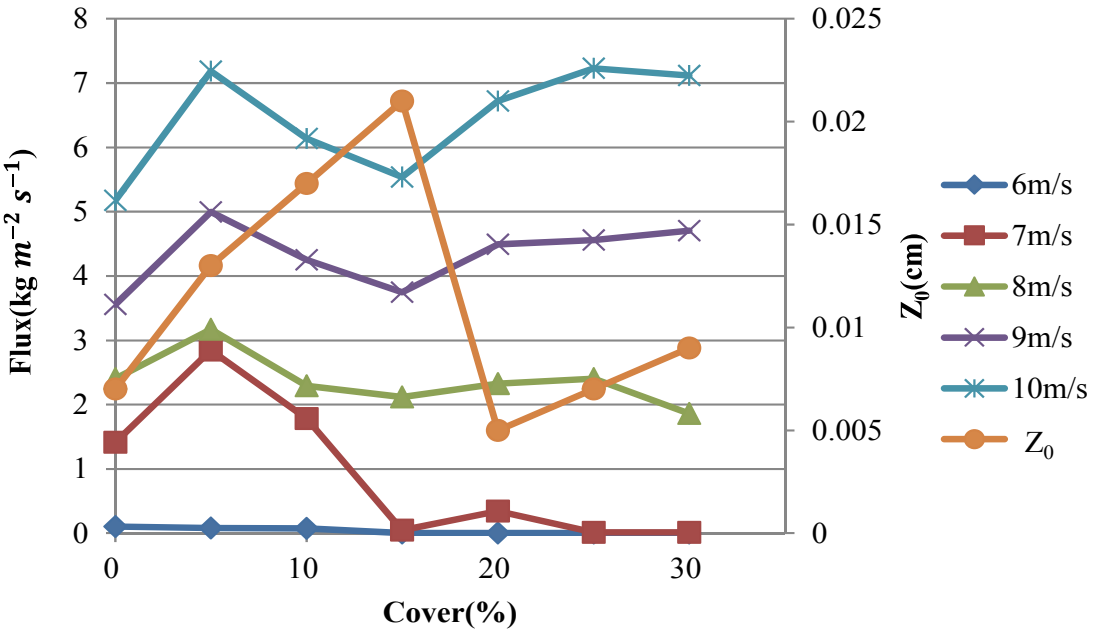

Fig 5.5 Comparison between the roughness length and the blown sand flux at a height of 8 cm for each coverage rate.

5.5 Conclusion

The occurrence of yellow sand in East Asia is said to be caused by saltation bombardment due to the particles having a particle size of 70 μm or more. The ground surface of the source of yellow sand is diverse and most of the Gobi desert in Mongolia is gravel. Despite the fact that the Gobi desert is the main source of yellow sand, there are only a few studies on how the gravel coverage influences the occurrence of blown sand and yellow sand, especially aerodynamically. In this study, we have examined the influence of gravel coverage rate on the vertical distribution of wind speed, roughness length and blown sand flux using a compact and simple wind tunnel and a piezoelectric blown sand meter and obtained the following results.

- Logarithmic law has been established for the vertical distribution of wind speed for the floor space with gravel of particle size (0.005 to 0.01 m).
- When the gravel coverage rate was in the range of 0% to 15%, the roughness length increased with an increase in the coverage rate. However, when it became 20% or more, the roughness length decreased to a value close to that at 0%.
- When the wind speed was weak (6 to 7 m/s), there was a trapping effect of blown sand at a gravel coverage rate of 15% or more.
- The range of influence is limited. Small gravel (particle size 0.005 to 0.01 m; corresponding to the size of gravel in the Gobi desert) used in this study can influence only the sand blown up to a height of 5 cm.
- Although an increase in the roughness length due to gravel coverage rate has the effect of decreasing the blown sand flux at a height of 8 cm, when the coverage rate became 20% or more, the ground surface became aerodynamically smooth and the blown sand flux at a height of 8cm began to increase again.

Thus, it can be considered that depending on the gravel coverage rate, the source of yellow sand containing gravel has a complex influence on the occurrence of blown sand and yellow sand. For example, it is interesting to know the influence of the blown sand flux at the height of 8 cm obtained in this study on the occurrence of yellow sand. In the future, in addition to verifying the results of this study by measuring the gravel coverage rate, blown sand flux and dust density in the source of yellow sand containing gravel, we wish to use these for the measures against the source of dust.

6. Conclusions and future requirements

Asian dust storms are natural phenomena that can cause severe ecological and environmental problems, affecting agriculture, human and animal health, land degradation, and desertification. The main source for these severe dust events in arid and semiarid regions of northeast Asia are Taklimakan Desert, Loess Plateau region, and Gobi Desert of China and Mongolia, respectively. Crucial needs for dust restraint countermeasures and an early warning system, which may be combined with weather forecasts of wind speed, would be helpful in preventing serious damage. However, for development of countermeasures and warning system, the relationship between dust outbreaks and surface condition has not been clarified yet. Especially, the effects of stone on the size distribution of saltating sand particles under natural conditions are poorly understood.

The important findings and conclusions of this study are listed below.

Chapter 3　On the boundary layer formation of a small simple type wind tunnel

By the combination use of Spire and Roughness block, a method for generating a boundary layer in a small wind tunnel was proposed. In the present study, it is not only adjusted to the air velocity distribution in the vertical direction or produced a boundary layer, but also proposed a method of adjusting the air velocity distribution uniformly in the horizontal direction. As a result, the boundary layer is obtained a thickness of 38 cm by 3.6 m rectifying distance. In addition, by devising the arrangement of roughness block, it has become possible to equalize the air velocity distribution substantially in the horizontal direction. In the future, elucidation of sand particle motion like a saltation and Asian dust emission mechanisms is expected using simple wind tunnel developed in this study.

Chapter 4　A method to make a boundary layer with roughness length

Based on the results of Liu and Kimura (2016), we examined to generate the

boundary layer, roughness length close to the natural field, uniform distribution of wind speed toward the horizontal direction, and stable observation field of the simple type wind tunnel. Without changing the arrange of roughness block, we proposed to adjust only the shape and number of speyer. As a result, boundary layer and roughness length became 36 cm and 0.01 cm which was close to the natural condition. Additionally, it was possible to make the uniform wind speed toward the horizontal direction, and stable observation field regarding the wind speed distribution.

Chapter 5 Wind speed characteristics and blown sand flux of gravel surface

We investigated the influence of the variation in gravel coverage rate on the roughness length and the blown sand flux using a compact and simple wind tunnel together with a turbulence generator. Consequently, when the gravel coverage rate was in the range of 5% to 15%, the roughness length increased with an increase in the coverage rate. However, when the coverage rate reached 20% or more, the value of the roughness length became close to that of a floor surface of only sand. Regarding the blown sand flux, when the wind speed was 7 m/s or less, there was a trapping effect on the blown sand at a gravel coverage rate of 15% or more. However, when the wind speed reached 8 m/s or more, the effect of coverage rate faded and when the wind speed reached 10 m/s, the effect of gravel coverage supplementing the blown sand disappeared. The increase in roughness length due to the increase in the gravel coverage rate (5% to 15%) corresponded to a decrease in the blown sand flux within a height of 8 cm. However, the decrease in roughness length due to the increase in gravel coverage rate (20% to 30%) corresponded to an increase in the blown sand flux at a height of 8 cm. Therefore, it is suggested that when the gravel density becomes 20% or more, although the total blown sand flux at a height less than 8 cm decreases, the blown sand flux at a height of 8 cm alone remarkably increases due to aerodynamic smoothening

Abstract

Currently, deserts cover 31,400,000 square kilometers of the earth's surface. This figure amounts to 21% of the total land area on the earth's surface. In the past 20 years, desert regions have been expanding by an area of approximately 50,000 to 70,000 square kilometers per year due to the warming climate. The expansion of desert areas causes frequent occurrences of sandstorms. Sandstorms affect an increasingly wide area every year, affecting several billion people and causing up to 42 billion dollars of economic damage. In recent years, sand drift is occurring more and more often in China. Afflicted regions are distributed over a wide area, and the extent of damage has been increasing as well. According to statistics, the frequency of occurrence of strong sand drifts was 5 times in the 1950s, 8 times in the 1960s, 13 times in the 1970s, 14 times in the 1980s, and 23 times in the 1990s. These statistics clearly demonstrate that the frequency has been increasing.

In order to mitigate damage caused by sand drift, it is first necessary to identify the factors that cause this phenomenon. Scientists are hopeful that it will be possible to apply the results of this research and develop technologies for suppressing sand drifts. However, since experiments conducted outdoors are hampered by adverse measurement conditions due to irregular changes in the wind direction, it is difficult for researchers to analyze how sand drift occurs. On the other hand, conducting experiments in wind tunnels allows researchers to analyze the sand drift phenomenon more easily. However, it is difficult to recreate conditions similar to natural environments using wind tunnels. Generation of boundary layers is one example.

The goal of this research is to create thick turbulent boundary layers in settling chambers that are as short as possible using simple small-scale wind tunnels. We attempted to design and develop a low-cost small-scale simple wind tunnel in which the stability of the horizontal profile of the wind velocity is maintained while forming a boundary layer that is relatively thick by using the two types of turbulence generators discussed by Counihan (1969) and Standen (1972) and the empirical formulas published by Irwin (1981).

Firstly, by the combination use of Speyer and Roughness block, a method for generating a boundary layer in a small wind tunnel was proposed. In the present study, it

is not only adjusted to the air velocity distribution in the vertical direction or produced a boundary layer, but also proposed a method of adjusting the air velocity distribution uniformly in the horizontal direction. As a result, the boundary layer is obtained a thickness of 38 cm by 3.6 m rectifying distance. In addition, by devising the arrangement of Roughness block, it has become possible to equalize the air velocity distribution substantially in the horizontal direction. In the future, elucidation of sand particle motion like a saltation and Asian dust emission mechanisms is expected using simple wind tunnel developed in this study.

Secondly, based on the results of Liu and Kimura (2016), we examined to generate the boundary layer, roughness length close to the natural field, uniform distribution of wind speed toward the horizontal direction, and stable observation field of the simple type wind tunnel. Without changing the arrange of roughness block, we proposed to adjust only the shape and number of speyer. As a result, boundary layer and roughness length became 36 cm and 0.01 cm which was close to the natural condition. Additionally, it was possible to make the uniform wind speed toward the horizontal direction, and stable observation field regarding the wind speed distribution.

Thirdly, we investigated the influence of the variation in gravel coverage rate on the roughness length and the blown sand volume using a compact and simple wind tunnel together with a turbulence generator. Consequently, when the gravel coverage rate was in the range of 5% to 15%, the roughness length increased with an increase in the coverage rate. However, when the coverage rate reached 20% or more, the value of the roughness length became close to that of a floor surface of only sand. Regarding the blown sand volume, when the wind speed was 7m/s or less, there was a trapping effect on the blown sand at a gravel coverage rate of 15% or more. However, when the wind speed reached 8m/s or more, the effect of coverage rate faded and when the wind speed reached 10m/s, the effect of gravel coverage supplementing the blown sand disappeared. The increase in roughness length due to the increase in the gravel coverage rate (5% to 15%) corresponded to a decrease in the blown sand volume within a height of 8cm. However, the decrease in roughness length due to the increase in gravel coverage rate (20% to 30%) corresponded to an increase in the blown sand volume at a height of 8cm. Therefore, it is suggested that when the gravel density becomes 20% or more, although

the total blown sand volume at a height less than 8cm decreases, the blown sand volume at a height of 8cm alone remarkably increases due to aerodynamic smoothening.

Abstract in Japanese

「飛砂実験のための小型簡易風洞の開発とその応用」

現在，世界の砂漠面積は約3140万平方キロメートルであり，陸地総面積の21％を占めている。過去20年間，気候の温暖化によって，毎年5-7万平方キロメートルの割合で砂漠化が拡大している。その結果，頻繁な砂嵐が発生し，その被害を受ける範囲が毎年拡がっており，数十億の人々が影響を受け，最大420億ドルの経済的損失をもたらしている。近年，中国でも飛砂の発生は増加している傾向があり，被害地は広く分布し，被害の程度も大きくなっている。統計によると，強い飛砂の発生頻度は，50年代は5回，60年代は8回，70年代は13回，80年代は14回，90年代は23回であり，明らかに増加傾向を示している。

飛砂の被害を軽減するためには，まず飛砂の発生要因を解明することが重要である。そして，その研究結果を利用し，飛砂の効果的な抑制技術を開発することが期待されている。しかしながら，野外の実験においては，風向が不規則に変化する等の観測条件の制約があるため，飛砂の基本的な発生過程の分析は難しい。一方，風洞を使って実験すれば，現象は分かり易く分析できるが，自然な環境と近い条件を再現することが難しい場合がある。例えば，境界層の生成が挙げられる。

本研究では，簡易な小型風洞を用いて，できるだけ短い整流場で厚い乱流境界層を実現することを目的とする。Counihan (1969)やStanden (1972)が考案した二種類の乱流発生器を基本として，Irwin (1981)が提示した経験式を利用し，小型風洞における比較的厚い境界層の形成と風速の水平分布の安定性を保持した安価な小型簡易風洞の設計，開発を試みた。

本論文では、第 1 に、スパイヤーとラフネスブロックを併用し、小型風洞で境界層を生成する方法について提案した。本研究では、鉛直方向の風速分布を調整し、境界層を生成するだけでなく、水平方向の風速分布を均等に調整する方法も提案した。その結果、境界層は 3.2 m の整流距離で 36 cm の厚さが得られた。また、スパイヤーの配置を工夫することにより、水平方向の風速分布をほぼ均等にすることが可能になった。今後は、本研究で構築された簡易風洞を、風紋や砂のサルテーション、黄砂発生メカニズム解明などの環境実験に応用することが期待される。

第2に、劉・木村(2017)が提示した簡易な小型風洞を基に,乱流調整装置（台形スパイヤーとラフネスブロック）を用いて,比較的厚い境界層の生成,自然界に近い粗度長,水平方向の均一な風速分布,風速の安定した観測場を同時に満たす方法・手順を提案した。その結果,ラフネスブロックの並べ方や密度を変更せず, 台形スパイヤーの形状や本数を工夫することにより,それらの実現が可能になった。

第3に、乱流発生器を併用した小型簡易風洞を使って、レキ被覆率の変化が粗度長と飛砂量に与える影響について検討した。その結果、レキ被覆率が5%から15%の範囲では、被覆率の増加に伴い、粗度長は増加した。しかし、被覆率が20%以上になると、砂のみの床面状態の粗度長の値に近くなった。飛砂量に関しては、風速が7 m/s以内では、レキ被覆率が15%以上で飛砂をトラップする効果があった。しかし、風速が8 m/s以上になると被覆率による効果は薄れ、風速が10 m/sになるとレキ被覆による飛砂補足の効果はほぼなくなった。レキ被覆率の増加（5%~15%）による粗度長の増加は、高さ8 cm以内の飛砂量の減少と対応していた。しかし、レキ被覆率の増加（20%~30%）による粗度長の減少は、高さ8 cmにおける飛砂量の増加に対応していた。このことから、レキ密度が20%以上になると、高さ8 cm未満のトータルな飛砂量は減少するが、空気力学的に滑らかになることで高さ8 cmにおける飛砂量だけが顕著に増加することが示唆された。

Supporting publications

- Liu J.Q. and Kimura R.: Study on the boundary layer formation of a small simple type wind tunnel. *Sand Dune Research*, 63 (3): 113-119,2017-02 (Chapter 3)

- Liu J.Q. and Kimura R.: Development of the method to make a boundary layer with roughness length close to the natural condition in the simple type wind tunnel. *Sand Dune Research*, 64 (1): 1-8,2017-08 (Chapter 4)

References

Abulaiti A, Kimura R. 2011. Characteristics of the Sand Drifting of Tottori Sand Dune in Springtime. *Sand Dune Research* **58** (2): 31-40.

Abulaiti A, Kimura R, Shinoda M. 2013. Vegetation effect of on sand transport in Mongolian grassland . *Sand Dune Research*, **59** (3): 117-128.

Bagnold RA. 1936. The movement of desert sand. *Proceedings of the Royal Society* **157:** 594-620.

Bagnold GA. 1937. The transport of sand by wind. *Journal of Geographical Sciences* **89**: 409-438.

Bagnold R. 1941. *The Physics of Blown Sand and Desert Dunes*. Methuen, London.

Belly PY. 1964. *Sand movement of wind*. Tech. Memo. U.S. Army Coastal Eng. Res. Cent., Washington D. C. **1:** pp. 80.

Betzer PR, Carder KL, Duce RA, Merrill JT, Tindale NW, Uematsu M, Costello DK, Young RW, Feely RJ, Breland JA, Bernstein RE, Greco AM. 1988. Long-range transport of giant mineral aerosol-particles. *Nature* **336**: 568-571

Bisal F, Hsieh J. 1966. Influence of moisture on erodibility of soil by wind. *Soil Science* **102** : (3) 143-146.

Butterfield G.: Near-bed mass flux profiles in Aeolian sand transport, high resolution measurements in a wind tunnel, *Earth Surface Processes and Landform*, 1999,24:393-412.

Cermak J.:Wind tunnel design for physical modeling of atmospheric boundary layers, *J.Eng.Mech.Dix.*,ASCE,1981,107(3):523-642.

Cermak J.E., Cochran L.S.: Physical Modeling of the Atmospheric Surface Layer, *Journal of Wind Engineering and Industrial Aerodynamics*.1992, 42(1-3), 935-946.

Chen W, Dong Z, Li Z, Yang Z. 1996. Wind tunnel test of the influence of moisture on the erodibility of loessial sandy loam soils by wind.

Journal of Arid Environments 34: 391-402.

Chen MX. 1990. Analysis of the hydrological system of Hexi Corridor, Gansu Province. *The Hydrological Basis for Water Resources Management*. **197**: 3-10.

Chen W, Fryrear DW, Yang Z. 1999. Dust fall in the Taklamakan Desert of China. *Physical Geography* **20**: 189-224.

Chepil WS. 1956. Influence of moisture on erodibility of soil by wind. *Soil Science Society of America Journal* **20**: 288- 292.

Chigira M, Yokoyama O. 2005. Weathering profile of non-welded ignimbrite and the water infiltration behavior within it in relation to the generation of shallow landslides. *Journal of Engineering Geology* **78**: 187-207.

Chimgee D, Shinoda M, Tachiiri K, Kurosaki Y. 2010. Why did a synoptic storm cause a dramatic damage in a limited area of Mongolia? *Journal of Mongolian Population* **19**: 63-68.

Chun Y, Boo KO, Kim J, Park SU, Lee M. 2002. Synopsis, transport, and physical characteristics of Asian dust in Korea. *Journal of Geophysical Research* **106** (D16): 18461-18469.

Chung YS, Kim HS, Park KH, Jhun JG, Chen SJ. 2003. Atmospheric loadings, concentrations and visibility associated with sandstorm: satellite and meteorological analysis. *Water Air Soil Pollution Focus* **3**: 21-4.

Ci LJ. 2002. Disasters of strong sandstorms over large areas and the spreadof land desertification in China. In Yang Youlin, Victor Squires & Lu Qi (Eds.), Global Alarm: *Dust and Sandstorms from the World's Drylands* 215-254.

CMA (China Meteorokogical Administration). 2002. Web page in April, 2992, www.cma.gov.cn.

Counihan, J. : An improved method of simulating an atmospheric boundary layer in a wind tunnel, *J. Fluid Mechanics*, vol. 3, pp. 197-214(1969)

Crawley DM, Nickling WG. 2003. Drag partition for regularly-arrayed rough

surface. *Boundary Layer Meteorology* **107**:445-468.

Dong F., Liu D.Y : Research progress and development trend of sand movement [J].*Advances in Mechanics*, 1995, 25 (3): 368-391.

Dong ZB, Gao SY, Fryrear AW. 2001. Drag coefficients, roughness length and zero-plane displacement height as disturbed by artificial standing vegetation. *Journal of Arid Environments* **49**: 485-505.

Dong ZB, Man DQ, Luo WY, Qian GQ, Wang JH, Zhao M, Liu SZ, Zhu GQ, Zhu SJ. 2010. Horizontal aeolian sediment flux in the Minqin area, a major source of Chinese dust storms. *Geomorphology* **116**: 58-66.

Etyemezian V, Nikolich G, Ahonen S, Pitchford M, Sweeney M, Purcell R, Gillies J, Kuhns H. 2007. The portable In Situ wind erosion laboratory (PI-SWERL): A new method to measure PM10 windblown dust properties and potential for emissions. *Journal of Atmospheric Environment* **41**: 3789- 3796.

Fe´can F, Marticorena B. Bergametti G. 1999. Parameterization of the increase of the aeolian erosion threshold wind friction velocity due to soil moisture for arid and semi-arid areas. *Annales Geophysicae* **17**: 149-157.

Gao Y, Arimoto R, Duce RA, Zhang XY, Zhang GY, An ZS, Chen LQ, Zhou MY, Gu DY. 1997. Temporal and spatial distributions of dust and its deposition to the China Sea. *Tellus* **49**B: 172-189.

Gillette D, Walker T. 1977. Characteristics of airborne particles produced by wind erosion on sandy soil, high plains of West Texas. *Soil Science* **123**: 97-110.

Gillies JA, Nickling WG, King J. 2007. Shear stress partitioning in large patches of roughness in the atmospheric inertial sublayer. *Boundary Layer Meteorology* **122**: 367-396.

Gong S, Zhang XY, Zhao TL, McKendry IG, Jaffe DA, Lu NM. 2003. Characterization of soil dust aerosol in China and its transport and distribution during 2001 ACE-Asia: 2. model simulation and

validation. *Journal of Geophysical Research* **108**: 4262, doi: 10.1029/2002JD002, 633.

Hagen LJ, Armbrust DV. 1994. Plant canopy effects on wind erosion saltation. *Transactions of the American Society of Agricultural Engineers* **37**(2): 461-465.

Hai B, Tie X, Cao JJ, Ying Z, Han SQ. 2011. Analysis of a Severe Dust Storm Event over China: Application of WRF-Dust model, Aero. *Air Quality Research* **11**: 419-428.

Ham, H.J., and Bogusz, B. : Wind tunnel simulation of TTU flow and building roof pressure, *Journal of Wind Engineering and Industrial Aerodynamics* ,77,119-133(1998)

Hill, Kara. J : Research on Preventing and Remediating the Dust Storms of China: A Case Study Investigating the Development of Salt Water Agriculture, *The Department of East Asian Languages and Literatures*, 7-14(2011)

Hoffmann C, Funk R, Wieland R, Li Y, Sommer M. 2008. Effects of grazing and topography on dust flux and deposition in the Xilingele grassland, Inner Mongolia. *Journal of Arid Environments* **72**: 792-807.

Ing GKT. 1972. A dust storm over central China, April 1969. *Weather* **27**: 136-145.

Intergovernmental Panel on Climate Change (IPCC), 2007. Climate change 2007, the Physical Science Basis. Cambridge University Press, Cambridge. pp. 989.

Irwin, H. P. A. H. : The design of spires for wind simulation, *Journal of Wind Engineering and Industrial Aerodynamics*,7,361-366(1981)

Ishizuka M, Mikami M, Yamada Y, Zeng F, Gao W. 2005. An observational study of soil moisture effects on wind erosion at a gobi site in the Taklimakan Desert. *Journal of Geophysical Research* **110**: D18S03.

Jugder D, Chung YS, Batbold A. 2004. Cyclogenesis over the territory of Mongolia during 1999–2002. *Journal of the Korean Meteorological Society* **40**: 3, 293-303.

Kawamura R. 1964. Study of sand movement by wind. In: Hydraulic Eng. Lab.Tech. Rep., University of California, Berkeley, CA HEL-2-8, pp. 99-108.

Kimura R, Bai L, Wang J. 2009. Relationships among dust outbreaks, vegetationcover, and surface soil water content on the Loess Plateau of China. *Catena* **77**: 292-296.

Kimura R, Shinoda M. 2010. Spatial distribution of threshold wind speeds for dust outbreaks in northeast Asia. *Geomorphology* **114**: 319-325.

King J, Nickling WG, Gillies JA. 2006. Aeolian shear stress ratio measurements within mesquite-dominated landscapes of the Chihuahuan Desert, New Mexico, USA. *Geomorphology* **82**: 229–244.

Kurosaki Y, Mikami M. 2003. Recent frequent dust events and their relation to surface wind in East Asia. *Geophysical Research Letters* **30** (14): 1736. doi:10.1029/2003GL0.

Kurosaki Y, Mikami M. 2005. Regional difference in the characteristic of dust event in East Asia: Relationship among dust outbreak, surface wind, and land surface condition. *Journal of the Meteorological Society of Japan* **83**: A, 1-8.

Lancaster N, Baas A. 1998. Influence of vegetation cover on sand transport by wind: field studies at Owens Lake, California. *Earth Surface Processes and Landforms* **23**: 69-82.

Laurent B, Marticorena B, Bergametti G, Chazette P, Maigan F, Schmechtig C. 2005. Simulation of the mineral dust emission frequencies from desert areas of China and Mongolia using an aerodynamic roughness length map derived from the POLDER/ADEOS 1 surface products. *Journal of Geophysical Research* **110**: D, doi:10.1029/2004JD005013.

Lettau K, Lettau HH. 1978. Experimental and micrometeorological field studies of dune migration. In: Lettau HH, Lettau K (eds) Exploring the World's Driest Climate, University of Wisconsin, Madison, WI,

pp. 110-147.

Li A , Shao Y. 2003. Numerical simulation of drag partition over rough surface. *Boundary Layer Meteorology* **108**: 317-342.

Li XL, Zhang HS. 2011. Research on threshold friction velocities during dust events over the Gobi Desert in northwest China. *Journal of Geophysical Research* **116**: D20.

Liu J.J, Zheng YF, Li ZQ, Flynn C, Welton EJ, Cribb M. 2011.Transport, vertical structure and radiative properties of dust events in southeast China determined from ground and space sensors. *Atmospheric Environment* **45**: 6469-6480.

Liu J.Q. and Kimura R.: Study on the boundary layer formation of a small simple type wind tunnel. *Sand Dune Research*, 63 (3): 113-119,2017-02

Liu J.Q. and Kimura R.: Development of the method to make a boundary layer with roughness length close to the natural condition in the simple type wind tunnel. *Sand Dune Research*, 64 (1): 1-8,2017-08

Ma Y. 1990. Flora intramongolica, typis intramongolicae popularis, huhhot. **2**: 759.

Marshall JK. 1971. Drag measurements in roughness arrays of varying density and distribution. *Journal of Agricultural Meteorology* **8**: 269-292.

McKenna-Neuman C, Nickling WG. 1989. A theoretical and wind tunnel investigation of the effect of capillarity water on the entrainment of sediment by wind. *Canadian Journal of Soil Science* **69**: 79-96.

Mehta,R.D. : The aerodynamic design of blower tunnels with wide-angle diffusers, *Progress of Aerospace Science*,18,59-94(1977)

Middleton NJ. 1991. Dust storms in the Mongolian People's Republic. *Journal of Arid Environments* **20**: 287-297.

Mikami M, Yamada Y, Ishizuka M, Ishimaru T, Gao W, Zeng F. 2005. Measurement of saltation process over Gobi and sand dunes in the Taklimakan Desert, China, with newly developed sand particle

counter. *Journal of Geophysical Research* **110**: D18S02, doi: 10.102 /2004JD004688.

Nakano T, Nemoto M, Shinoda M. 2008. Environmental controls on photosynthetic production and ecosystem respiration in semi-arid grasslands of Mongolia. *Agricultural and Forest Meteorology* **148**: 1456-1466.

Natsagdorj DL, Jugder D, Chung YS. 2003. Analysis of dust storms observed in Mongolia during 1937-1999. *Atmospheric Environment* **37**: 1401-1411.

Nickling W, Gillies J. 1993. Dust emission and transport in Mali, West Africa. *Sedimentology* **40**: 859-868.

Okada K, Kai K. 1995. Features and elemental composition of mineral particles collected in Zhangye, China. *Journal of the Meteorological Society of Japan* **73**: 947-957.

Oke TR. 1978. *Boundary Layer Climates*. Methuen & Co Ltd., New York.

Owen P.R., Zienkiewicz H.K.: The Production of Uniform Shear Flow in a Wind Tunnel, *Journal of Fluid Mechanics*. 1969,36(2):367-383.

Oyafuso A, Ota M, Ishimine M, Arakaki N. 2011. Vertical distribution of female adults and larval offspring of the white grub Dasylepida ishigakiensis (Coleoptera: Scarabaeidae) in the soil of a sugarcane field on Miyako Island, Okinawa. *Japanese Society of Applied Entomology and Zoology* **46**: 171-176.

Owen RP. 1964. Saltation of uniform grains in air. *Journal of Fluid Mechanics* **20**: 225-242.

Pye K. 1987. Aeolian Dust and Dust Deposits. Academic Press, New York.

Qian WH, Quan L, Shi S. 2002. Variations of the dust storm in China and its climatic control. *Journal of Climate* **15**: 1216-1229.

Raupach MR, Gillette DA, Leys JF. 1993. The effect of roughness elements on wind erosion threshold. *Journal of Geophysical Research* **98**: 3023-3029.

Schlichting H. 1936. Experimentelle untersuchungen zum rauhigkeitsproblem. *Ingen. Arch* **7**: 1-34.

Selah A, Fryrear DW. 1995. Threshold wind velocities of wet soils as affected by wind blown sand. *Soil Science* **160**: (4) 304-309.

Shao Y, Raupach M, Findlater P. 1993. The effect of saltation bombardment on the entrainment of dust by wind. *Journal of Geophysical Research* **98**: 12719-26.

Shao Y, Raupach MR, Leys JF. 1996. A model for predicting Aeolian sand drift and dust entrainment on scales from paddock to region. *Australian Journal of Soil Research* **34**: 309-342.

Shao Y. 2000. A simple expression for wind erosion threshold friction velocity. *Journal of Geophysical Research* **105**: 437-443.

Shao Y, Mikami M. 2005. Heterogeneous saltation: theory, observation and comparison. *Boundary Layer Meteorologyogy* **115**: 359-379.

Shao Y, Dong CH. 2006. A Review on East Asian Dust Storm Climate, Modelling and Mornitoring. *Global and Planetary Changes* **52**: 1-22.

Shao Y. 2008. *Physics and Modeling of Wind Erosion*, Vol. 37 of Atmospheric and Oceanographic Sciences Library. Kluwer Academic Press, Dordrecht, Netherlands.

Sill B.L. : Turbulent boundary layer profiles over uniform rough surfaces, *Journal of Wind Engineering and Industrial Aerodynamics*,31(2),147-163(1988)

Shinoda M, Ito S, Nachinshonhor GU, Erdenersetseg D. 2007. Phenology of Mongolian grasslands and moisture conditions. *Journal of the Meteorological Society of Japan* **85:** 359-367.

Shinoda M, Nachinshonhor GU, Nemoto M. 2010. Impact of drought on vegetation dynamics of the Mongolian steppe: a field experiment. *Journal of Arid Environments* **74:** 63-69.

Shinoda M, Gillies JA, Mikami M, and Shao Y. 2011. Temperate grasslands as a dust source: Knowledge, uncertainties, and challenges. *Aeolian Research* **3(3)**: 271-293. doi:10.1016/j.aeolia.2011.07.001.

Siddoway FH, Chepil WS, Armbrust DV. 1965. Effect of kind, amount, and placement of residue on wind erosion control. *Journal of Fluids*

Engineering **8**: 327-331.

Standen N.M. : A Spire Array for Generating Thick Turbulent Shear Layers for Natural Wind Simulation in Wind Tunnels, National Research Council of Canada, *NAE*, LTR-LA-94(1972)

Su YZ, Wang F, Zhang ZH, Du MW. 2007. Soil Properties and Characteristics of Soil Aggregate in Marginal Farmlands of Oasis in the Middle of Hexi Corridor Region, Northwest China. *Agricultural Sciences in China* **6**(6): 706-714.

Sun XY, Xiao Y, Chang XL, Zhang N, Han Y, Ji XX. 2011. Patch dynamics of cropland and grassland in Zhangye oasis, Gansu Province in recent two. *Chinese Journal of Ecology* **30**(6):1198-1203. (in Chinese)

Tan,L.and W.Zhang : Aeolian sand transport over gobi with different gravel coverages under limited sand supply, *A mobile wind tunnel investigation, Aeolian Research*,11,67-74(2013)

Thorsteinsson T, Gísladóttir G, Bullard J, McTainsh G. 2011. Dust storm contributions to airborne particulate matter in Reykjavík, Iceland. *Atmospheric Environment* **45**: 5924-5933.

Tian L.H., Zhang W.M., Qu J.J., Zhang K.C., An Z.S., Wang.X: Aeolian sand transport over gobi with different gravel coverages under limited sand supply, A mobile wind tunnel investigation, *Aeolian Research*, Volume 11, December 2013, Pages 67-74.

UNEP. 1997. World Atlas of Desertification. Arnold, London. pp. 182.

Ushiyama I. 2002. *Windmill Engineering Introduction*. Morikita Shuppan (in Japanese).

Wang XM, Dong ZB, Zhang JW. 2004. Modern Dust Storms in China: An Overview. *Journal of Arid Environments* **58**: 559-574.

Wang Y., Zhang H.Y.:The study on similarity parameters of the atmospheric surface layer and phenomena of drift sand[J]. *Journal of Desert Research*, 1994, 14(1): 10 －16. (in Chinese with English abstract)

White B.R.: Laboratory simlation of eolian sand transport and physical modeling of flow around Dounes, *Annals of Arid*

zone,1996,35(3):187-213

Willis DM, Easterbrook MG, Stephenson FR. 1980. Seasonal variation of oriental sunspot sightings. *Nature* **287**: 617-619.

Wolfe SA, Nickling WG. 1993. The protective role of sparse vegetation in wind erosion. *Progress in Physical Geography* **17**: 50-68.

Wu Z. 2003. Geomorphology of Wind-Drift Sands and Their Controlled Engineering. Science Press, Beijing. 448 pp. (in Chinese).

Wyatt VE, Nickling WG. 1997. Drag and shear stress partitioning in sparse desert creosote communities. *Canadian Journal of Earth Sciences* **34**: 1486-1498.

Yamada Y, Mikami M, Nagashima H. 2002. Dust particle measuring system for streamwise dust flux. *Journal of Arid Land Studies* **11**(4): 229-234.

Yamamoto T, Yoshino M, Suzuki J. 2007. The relationship between occurrence of dust events and synoptic climatological condition in East Asia. 1999-2003. *Journal of the Meteorological Society of Japan* **85**: 81-99.

Yamamoto T. 2008. Soil degradation and its rehabilitation in arid region. Kokon Shoin press, Tokyo, Japan. pp. 262.

Yang Y, Shao Y. 2005. Drag partition and its possible implications for dust emission. *Water, Air, and Soil Pollution* **5**: 251-259.

Youngsin C, Lim JY. 2003. The recent characteristics of Asian dust and haze events in Seoul, Korea. *Meteorology and Atmospheric Physics* **10**: 10.1007/s00703-003-0067-2.

Yuan CS, Sau CC, Chen MC, Hunag MH, Chang SW, Lin YC, Lee CG. 2004. Mass concentration and size-resolved chemical composition of atmospheric aerosols sampled at the Pescadores Islands during Asian dust storm periods in the years of 2001 and 2002. *Terrestrial Atmospheric and Oceanic Sciences* **15**: 857-879.

Zhang XY, Arimoto R, An ZS. 1997. Dust emission from Chinese desert sources linked to variations in atmospheric circulation. *Journal of*

Geophysical Research **102**(D23): 28041-28047.

Zhang XY, Arimoto R, Zhu GH, Chen T, Zhang GY. 1998. Concentration, size-distribution and deposition of mineral aerosol over Chinese desert regions. *Tellus* **50**B:317-330.

Zhang Q, Zhao X, Zhao H. 1998. Grasslands in Desert Area of China. Meteorology Press, Beijing, 1-10.

Zhao M, Zhan KJ, Yang ZH, Fang ET, Qiu GY, Wang QQ, Zhang YC, Guo SJ, Li AD, Zhang JC. 2011. Characteristics of the lower layer of sandstorms in the Minqin desert-oasis zone. *Science China Earth Sciences* **54**: 703-710.

Zheng J, He M, Li X, Chen Y, Li X, Liu L. 2008. Effects of Salsola passerina shrub patches on the microscale heterogeneity of soil in a montane grassland, China. *Journal of Arid Environments* **72**: 150-161.

Zingg AW. 1953. Wind-tunnel studies of the movement of sedimentary material. In: Proceedings of the 5th Hydraulic Conference, University of Iowa Studies in Engineering, Iowa City, IA, **34**. pp. 111-135.